NATIONAL ADVISORY COMMITTEE FOR AERONAUTICS

TECHNICAL NOTE 2578

A COMPARISON OF PREDICTED AND EXPERIMENTALLY DETERMINED LONGITUDINAL DYNAMIC RESPONSES OF A STABILIZED AIRPLANE

By Louis H. Smaus, Marvin R. Gore,
and Merle G. Waugh

Ames Aeronautical Laboratory
Moffett Field, Calif.

Washington
December 1951

TABLE OF CONTENTS

NATIONAL ADVISORY COMMITTEE FOR AERONAUTICS

TECHNICAL NOTE 2578

A COMPARISON OF PREDICTED AND EXPERIMENTALLY DETERMINED LONGITUDINAL DYNAMIC RESPONSES OF A STABILIZED AIRPLANE

By Louis H. Smaus, Marvin R. Gore,
and Merle G. Waugh

SUMMARY

The dynamic longitudinal stability of an airplane with autopilot was predicted by combining the transfer functions of the autopilot obtained from tests made on the ground with those of the airplane measured in flight to obtain the open- and closed-loop frequency responses and transient responses for the combination. These predicted responses were then compared with measured flight frequency and transient responses for three airspeeds and various autopilot settings of displacement and rate of displacement feedback. The analysis procedures were based upon linear methods and agreement was good when elements were operated in flight within the linear range except for certain conditions in which rate of displacement feedback was used.

INTRODUCTION

The purpose of the investigation was to determine how well the longitudinal dynamic stability of an autopilot-aircraft combination could be predicted from the separately measured characteristics of the autopilot and of the aircraft. The methods of analysis were based on standard servomechanism theory as exemplified by reference 1. A general survey of the methods of predicting the dynamic response for an autopilot-aircraft combination is given in reference 2. Most of the specific equations used in this analysis and the manner of diagramming the closed-loop system were developed in reference 3.

The transfer functions obtained experimentally for the aircraft and for the autopilot were multiplied together and the resulting open-loop frequency response was plotted on a conventional Nyquist diagram to indicate the relative stability. The closed-loop frequency response, that is, the ratio of pitch response to a sinusoidal disturbance in pitch for the autopilot-aircraft combination, was then calculated

directly from the open-loop response. In addition, the transient responses to step input disturbances were calculated by an approximation method. These three predicted responses were compared with those measured in flight, the transient response and the closed-loop frequency response having been measured directly for step and sinusoidal inputs, respectively, and the open-loop response derived analytically from the closed-loop response. Calculations and measurements were made for airspeeds of 85, 130, and 200 knots and for various autopilot settings of displacement and rate of displacement feedback.

DEFINITIONS AND SYMBOLS

Frequency response: A frequency-dependent vector response of the output of a system to a sinusoidally varying input function, expressed quantitatively by a plot of amplitude ratio and phase angle versus frequency.

Amplitude ratio: The ratio of the output amplitude to the input amplitude. For a closed-loop system this is ordinarily nondimensiomalized by dividing by the amplitude ratio at zero frequency.

Phase angle: The angle between an output vector and input vector. When the output leads the input, the angle is positive.

Transfer function: The expression defining the ratio of the output of a component to the input, usually expressed as a complex function of the frequency variable f.

Closed-loop response: The frequency response of a closed-loop system, that is, one which possesses feedback and is sensitive to the difference between output and input.

Open-loop response: The frequency response of an open-loop system.

Servo system: That part of the autopilot composed of the amplifier and servo actuator or motor and its internal feedback loop.

Autopilot: The airplane stabilizing system composed of the servo system and the feedback gyros.

Voltages, angular displacements, and transfer functions are vector quantities having amplitudes and phase angles unless otherwise noted.

A_L open-loop transfer function of autopilot-aircraft combination

$$\left(\frac{v_g+v_r}{v_i}\right) \text{ or } \left(\frac{\theta+\theta_r}{\theta_i}\right)$$

A_p transfer function of servo system, nondimensionalized

A_r transfer function of rate gyro

A_θ transfer function of aircraft in pitch $\left(\frac{\theta}{\delta}\right)$

e 2.718...

f frequency, cycles per second

j $\sqrt{-1}$

k_f follow-up pickoff constant, volts per degree

k_g displacement gyro constant, volts per degree

k_p static control gearing, ratio of control surface deflection to angular displacement input to autopilot, degrees per degree

k_r rate gyro constant, volts per cycle per second per degree oscillation

P_f gain of follow-up attenuator, also referred to as sensitivity, percent

P_r gain of rate gyro attenuator, percent

R amplitude ratio of servo-system frequency response A_p, dimensionless

R_{fr} amplitude ratio of autopilot frequency response when rate of displacement input signal is included $\left(A_p \frac{1+P_r A_r}{k_g}\right)$, dimensionless

v_e error signal of servo system (input to amplifier) when the servo system is tested with displacement input signal only, volts

v_{er} error signal of servo system (input to amplifier) when the servo system is tested with both displacement and rate of displacement input signals, volts

v_{ec} error signal of servo system (input to amplifier) when the autopilot-aircraft closed-loop combination is tested, volts

v_E error signal of autopilot-aircraft combination (v_I-v_g), volts

v_f feedback voltage of servo system, volts

v_{fr} feedback voltage of servo system when tested with both displacement and rate of displacement input signals, volts

v_g displacement gyro output, volts

v_i input signal to the servo system, volts

v_I input signal to the autopilot-aircraft combination, volts

v_r rate gyro output, modified by rate attenuator, volts

δ_e control surface deflection, degrees

δ_s servo displacement, inches

ϵ_e phase angle of v_e relative to v_i, degrees

ϵ_{er} phase angle of v_{er} relative to v_i, degrees

ϵ_f phase angle of servo-system frequency response A_p, v_f relative to v_i, degrees

ϵ_{fe} phase angle of v_f relative to v_e, degrees

ϵ_{fr} phase angle of autopilot frequency response $\left(A_p \frac{1+P_r A_r}{k_g}\right)$ when rate of displacement input signal is included, equivalent to phase angle of v_{fr} relative to θ, degrees

ϵ_L phase angle of open-loop autopilot-aircraft combination A_L, (v_g+v_r) relative to v_i (and $(\theta+\theta_r)$ relative to θ_i), degrees

ϵ_r phase angle of v_r relative to θ, degrees

θ angular displacement, attitude of aircraft, degrees

θ_E error angle, degrees

θ_i hypothetical input angle to servo system, degrees

θ_I input angle to autopilot-aircraft combination, degrees

θ_r hypothetical rate feedback angle, degrees

See diagram page 11

DESCRIPTION OF TEST EQUIPMENT

Airplane

The airplane used in these tests was a conventional propeller-driven Navy dive bomber which was equipped for automatic control. A photograph is presented in figure 1.

A control cable and pulley system connected the elevator and control stick. The autopilot servo actuator was attached at the control stick end of this linkage.

Autopilot

Automatic control of the airplane about all axes was furnished by a commercially manufactured autopilot modified to include rate gyros. A photograph of the basic components of the pitch channel of the system is shown in figure 2. A displacement or vertical gyro is used to sense pitch angle. A rate gyro senses pitching angular velocity. The servo system produces an elevator deflection in accordance with the gyro outputs and includes the components described as follows. An amplifier converts the small electrical signals received from the gyros and follow-up pickoff to currents sufficiently large to operate the solenoid-controlled hydraulic transfer valve. The solenoid transforms the electric current to a mechanical motion, closing or opening ports, and thus controlling the flow of hydraulic fluid. A piston-type servo actuator converts the hydraulic flow to a linear motion having sufficient force to actuate the control surface of the airplane. The actuator is connected to the elevator cross member of the control-stick mechanism. A follow-up pickoff is attached to the piston output to produce an electrical signal proportional to displacement which is then fed back to the amplifier to complete the inner servo loop. This feedback is varied by means of the sensitivity control, a potentiometer controlling the input excitation to the follow-up pickoff. Variation of this control has the dual effect of changing the dynamic response of the servo system and changing the ratio of surface deflection to input signal which alters the response of the autopilot-aircraft combination.

A block diagram of the complete autopilot-aircraft loop is shown in figure 3. A potentiometer associated with the rate gyro allows variation of the amount of pitch-rate signal fed back. No such control is provided for the displacement gyro since a variation of the servo follow-up potentiometer effectively alters the pitch-angle feedback.

Instrumentation

The recording system for flight was centered about a six-channel Miller oscillograph. Servo and elevator surface positions were measured by means of rotatable transformers used as electrical pick-offs and lever arm linkages. Pitch angle was measured with a Sperry A-12 vertical gyro which has a similar pickoff. The alternating-current voltages from the position and attitude pickoffs were demodulated and recorded on the oscillograph. Rate of pitch was obtained from a rate gyro with a microsyn pickoff; the 400-cycle alternating-current voltage was recorded directly on the oscillograph without rectification. A separate galvanometer was used to record the current to the solenoid valve, this being a measure of the error voltage to the amplifier. A standard NACA airspeed-altitude recorder also was used.

For sinusoidal response tests the sine-wave input signal was obtained from a device in which a rotating selsyn was driven by a ball-disc variable-speed mechanism. The amplitude of the 400-cycle output voltage from the selsyn could be varied in frequency from 0 to 10 cycles per second. A contactor was operated once per cycle at a zero output voltage point, introducing a signal to the oscillograph which provided a zero-phase reference marker. The sine-wave amplitude was set and measured on the ground.

For transient-response tests pulses were introduced by a motor-driven potentiometer arrangement. Both amplitude and time base could be adjusted on the ground. Steps were obtained by a simple switch. The various input voltages were introduced in series with the other elements in the autopilot signal circuit and are indicated by the symbol v_I in figure 3.

For the ground tests of the servo system a Brush recorder was used to indicate servo and surface positions, and the zero-phase reference marker was superimposed on one of the traces.

THEORETICAL ANALYSIS

The method of predicting the dynamic response of the stabilized (autopilot-controlled) airplane is based on the determination and combination of the transfer functions of the aircraft and of the autopilot. The relative stability may then be ascertained from an inspection of the resultant open-loop frequency response, closed-loop frequency response, and transient response. These responses are mathematically related as shown subsequently, but each provides information on the relative stability not readily apparent from the others.

The Aircraft

Transient experimental flight data was the most important source of aircraft frequency-response characteristics. This information was obtained from flight film records by a method of analysis based upon the Fourier transform as outlined as follows.

For many considerations of dynamic stability the longitudinal motions of an airplane can be closely described by a second-order differential equation (reference 4). The quantities involved in the stabilization system of the test airplane, namely, the angle of pitch, θ, as controlled by the elevator position, δ, may be related by the equation

$$\frac{d^2\theta}{dt^2} + b\frac{d\theta}{dt} + k\theta = C_1\delta + C_o\int \delta\, dt$$

This differential equation may be converted by the Laplace transformation into its transfer-function form:

$$\theta(s) = \frac{C_1 s + C_o}{s(s^2+bs+k)}\,\delta(s) \qquad (1)$$

When θ and δ are known experimentally as functions of time, they can be converted into the s plane by the Laplace integrals

$$\theta(s) = \int_o^\infty \theta(t)e^{-st}dt$$

$$\delta(s) = \int_o^\infty \delta(t)e^{-st}dt$$

where $\theta(t)$ and $\delta(t)$ are assumed to be zero for all $t<0$.

Equation (1) can then be written

$$\int_o^\infty \theta(t)e^{-st}dt = \frac{C_1 s + C_o}{s(s^2+bs+k)} \int_o^\infty \delta(t)e^{-st}dt$$

The frequency response may now be calculated by replacing s by $j\omega$, where ω is any arbitrary value of angular frequency. (See reference 1.) Thus, frequency response is written:

$$\frac{\theta(j\omega)}{\delta(j\omega)} = \frac{C_1(j\omega)+C_o}{(j\omega)[(j\omega)^2+b(j\omega)+k]} = \frac{\int_o^\infty \theta(t)e^{-j\omega t}dt}{\int_o^\infty \delta(t)e^{-j\omega t}dt} \qquad (2)$$

The two integrals are called Fourier integrals and are usually directly calculable. When these integrals do not converge, limiting values may be obtained by replacing the integrals with the following more general form of the Laplace transformation in which $s = \sigma + j\omega$:

$$\theta(j\omega) = \lim_{\sigma \to o} \int_o^\infty \theta(t)e^{-(\sigma+j\omega)t}dt$$

Thus by equation (2), when θ and δ are known as functions of time, the frequency response may be computed for any arbitrary value of angular frequency, ω, by evaluating the two simple integrals above.

Considerable work can be saved if $\theta(t)$ and $\delta(t)$ are chosen so that the transient portions are short. (See fig. 4.) The integrals then involve statistical integration up to some time, T, when steady state is reached and an analytical expression will finish the evaluation of the integral from T to infinity. The statistical work is begun by dividing the interval $t = 0$ to $t = T$ into increments of about 0.1 second, and the integration is performed numerically, utilizing some approximation system such as Simpson's Rule.

This method for obtaining frequency-response functions from transient data is discussed in greater detail in reference 5.

The Autopilot

The characteristics of the autopilot and its components were obtained primarily by tests on the ground of the equipment while installed in the airplane. Since the predicted autopilot-aircraft response is theoretically valid only if the individual component responses are linear, the autopilot was examined with this consideration in mind.

The servo system is linear in operation only for input signals to the amplifier not exceeding a certain value. This nonlinearity results from saturation of the amplifier which has a static input-output relation as shown in the sketch. The amplifier input voltage is more coveniently referred to as the servo-system error voltage, v_e, as can be seen from figure 3. Thus it becomes necessary to know the error voltage to determine whether the servo system is operating within its linear range. The error voltage is, of course, a function of the input voltage to the servo system v_i as well as of the feedback voltage v_f from the servo output.

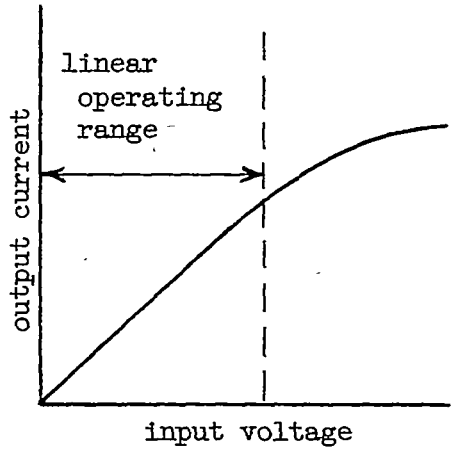

If the response of the servo system alone (without the gyros) is being considered, the input to the system is v_i. An expression for the error voltage in this case is given in reference 3, equation (5), and is

$$|v_e| = v_i \sqrt{1+R^2-2R \cos \epsilon_f} \tag{3}$$

where R and ϵ_f are, respectively, the nondimensional amplitude ratio and phase angle of the closed-loop servo-system response A_p.

When the response of the autopilot, that is, the control-surface response δ_e to an angular attitude input θ to the gyros, is considered, the error voltage v_{er} in this case is, from equation (12) of reference 3,

$$|v_{er}| = v_g \sqrt{\left(1-R_{fr} \cos \epsilon_{fr} + \frac{P_r k_r f}{k_g} \cos \epsilon_r\right)^2 + \left(R_{fr} \sin \epsilon_{fr} - \frac{P_r k_r f}{k_g} \sin \epsilon_r\right)^2} \tag{4}$$

where R_{fr} and ϵ_{fr} are, respectively, the nondimensional amplitude ratio and phase angle of the autopilot response when both rate and displacement gyros are oscillated. The term $P_r k_r f$ is the amplitude of the transfer function $P_r A_r$ for the rate gyro. The displacement gyro output, for practical purposes, is related to the input θ by a constant k_g.

From a knowledge of the servo-error voltage it is possible, in many instances, to choose input magnitudes small enough to insure operation of the servo in the linear range. This is not always the case, however,

and several of the test results presented herein involve the nonlinear range, but no attempt is made to calculate the effects of nonlinearity on the predicted results.

A second source of nonlinearity exists in the elevator linkage. Coulomb friction in the control-surface hinge and flexing of the pulley brackets and supporting deck are the probable causes.

Stability Criteria

Several criteria exist for determining stability. One of the most popular is based on the use of the Nyquist diagram which is explained fully in reference 1 and other references listed therein. Briefly, a polar plot in the complex plane is made of the open-loop frequency response. For the cases considered in this investigation, an encirclement of the $-1 + j0$ point represents an unstable system, whereas coincidence with the point represents a condition of neutral stability. The latter case is simply equivalent to saying that the output magnitude is the same as the input (the system gain is unity), but is 180° out of phase. Since the displacement feedback in a servo system is negative and, hence, has an additional 180° phase lag, it will lag a total of 360° and therefore add to the input signal. Therefore, any oscillations which may start are self-sustaining and the system will hunt indefinitely and with constant amplitude.

The nearness of the plot to the $-1 + j0$ point is an indication of the relative stability of the system and is often given in terms of gain and phase margins. Phase margin is defined as the angle between 180° and the point at which the open-loop response passes through the circle of unit magnitude. Gain margin is the reciprocal of the open-loop response magnitude when the phase angle is 180°. (See reference 1.) However, no simple quantitative relations correlate the Nyquist plot with characteristics of the transient response such as period and time to damp to a specified amplitude, except for a second-order system.

The closed-loop frequency response plot also gives an indication of the stability. The amplitude of the resonant peak is a rough measure of the damping, and the resonant frequency, if it clearly exists, is close to the transient frequency and the undamped natural frequency of the system.

Perhaps the final measure of stability is the transient response itself. Usually a particular form of this response is desired, often one that has an equivalent damping ratio in the neighborhood of 0.6 critical damping and a certain speed of response or natural frequency. These criteria may be modified by other limitations, such as the maximum allowable acceleration that may be imposed on personnel or airframe.

The Autopilot-Aircraft Loop

A block diagram of the autopilot-aircraft loop is given in figure 3. For purposes of analyzing the open-loop characteristics, the loop may be opened anywhere, but it is most convenient to break it between the aircraft output and the gyro input. The open-loop transfer function is then given in terms of a ratio of the pitch-angle output to a pitch-angle input. This is the function that is plotted on a Nyquist diagram. As previously stated, varying the amount of elevator deflection for a given vertical gyro displacement changes the gain of the over-all system. The change in amplitude on the Nyquist plot is, of course, proportional to the change in system gain, and, hence, directly affects the stability of the closed-loop combination.

A closed-loop response is obtained by inserting an input signal at some point and measuring an output response at any other point with the loop closed. The output generally of interest is, again, the pitch angle. It is then desirable to use a pitch input, but in flight it is impractical to feed in a sinusoidally varying pitch angle. Therefore, an equivalent pitch input is obtained by inserting a voltage, v_I, in the autopilot signal circuit (fig. 3). This voltage is related to the hypothetical pitch input then by the same constant, k_g, relating voltage output per degree input for the displacement gyro. The input for a transient response is introduced in the same manner.

Fundamental Relations

Relations between open-loop and closed-loop frequency responses are given generally in servomechanisms texts. The particular forms used herein were derived in reference 3 for application to the autopilot-aircraft combination. They are expressed in terms of the quantities actually measured during tests. In this connection, as is shown in reference 3, it is helpful to redraw figure 3 as follows:

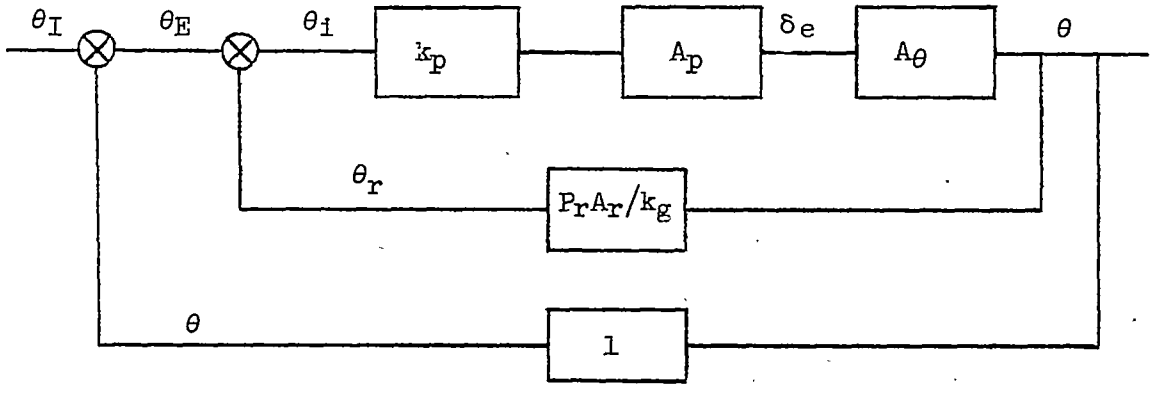

The equivalent angular input is θ_I (where $v_I \triangleq k_g \theta_I$) and the error angle is θ_E. The term k_p represents the autopilot gearing, the static ratio of elevator deflection to vertical gyro displacement. The nondimensional frequency response of the autopilot with the output measured at the control surface and without pitch-rate feedback is A_p. The relative amount of rate to displacement feedback is represented by the term $P_r A_r/k_g$ where A_r is the rate-gyro transfer function, P_r the rate attenuation factor, and k_g the vertical gyro constant. The aircraft response is A_θ.

It should be noted that all quantities are considered as vectors, possessing both magnitude and phase angle, unless otherwise noted. The term v_I, or its equivalent θ_I, is the reference and has zero phase angle.

The equations presented in the following paragraphs were used in the calculations involved in predicting and analyzing the performance of the autopilot-aircraft combination. They are presented without formal derivation and may be derived from the preceding diagram and elementary servo theory. For further details of these relations and others governing the calculation of servo-error voltage, servo response for a change of servo gain, and servo response with addition of rate of displacement input signal the reader is referred to reference 3.

Open-loop frequency response from closed-loop frequency response.- The open-loop response A_L may be calculated from the closed-loop response θ/θ_I as measured in flight from the equation

$$A_L = \frac{\left(\frac{\theta}{\theta_I}\right)\left(1 + \frac{P_r A_r}{k_g}\right)}{1 - \left(\frac{\theta}{\theta_I}\right)\left(1 + \frac{P_r A_r}{k_g}\right)} \tag{5}$$

From this it can be seen that in addition to measuring the closed-loop response it is necessary to evaluate the feed-back factor $(1 + P_r A_r/k_g)$. This can be done in two ways. If the transfer functions k_g and $P_r A_r$ for both displacement and rate gyros, respectively, are known, the factor may readily be calculated for the frequency range of interest.

On the other hand, if the frequency response of the autopilot servo system is known for a rate setting of zero and for the rate signal being considered, the feed-back factor may be obtained from the two responses. It may readily be seen from the foregoing sketch that the nondimensional autopilot dynamic response with rate signal present is the product of the servo-system response A_p and the feed-back factor $(1 + P_r A_r/k_g)$. (The gearing term k_p shown in the sketch is simply a constant which converts the nondimensional response to its absolute magnitude.)

Therefore the feed-back factor can be evaluated from the ratio of the rate response to no-rate response, or

$$\left(1 + \frac{P_r A_r}{k_g}\right) = \frac{\left[A_p \left(1 + \frac{P_r A_r}{k_g}\right)\right]_{\text{measured}}}{A_p} \tag{6}$$

Open-loop frequency response from autopilot and aircraft component responses.- The open-loop response is simply the product of the individual transfer functions around the loop.

$$A_L = k_p A_p \left(1 + \frac{P_r A_r}{k_g}\right) A_\theta \tag{7}$$

As was shown previously, the term $A_p(1 + P_r A_r/k_g)$ represents the nondimensional response of the autopilot servo system with rate-of-displacement signal added and may be measured directly. Or, if more convenient, the feed-back factor $(1 + P_r A_r/k_g)$ may be calculated from the gyro transfer functions.

Closed-loop frequency response from open-loop frequency response.- The closed-loop response θ/θ_I cannot be calculated directly from the open-loop response alone but must take into account the feedback due to the rate gyro. Hence,

$$\frac{\theta}{\theta_I} = \frac{k_p A_p A_\theta}{1 + k_p A_p A_\theta \left(1 + \frac{P_r A_r}{k_g}\right)} \tag{8}$$

In terms of the open-loop response from equation (7) and the feed-back factor, the above equation may be rewritten as

$$\frac{\theta}{\theta_I} \quad \frac{A_L}{\left(1 + \frac{P_r A_r}{k_g}\right)\left(1 + A_L\right)} \tag{9}$$

Error voltage for the autopilot-aircraft combination.- The servo-system error voltage has been discussed previously in connection with tests of the components. When it is desired to predict the autopilot-aircraft-combination response, it is again necessary to calculate

the error voltage for the input signal being considered in order to determine whether the amplifier is operating within its linear range. The expression for the error voltage in this case, designated v_{ec}, is, from reference 3, equation (42),

$$|v_{ec}| = v_I \sqrt{\frac{1+R^2-2R\cos\epsilon_f}{1+|A_L|^2+2|A_L|\cos\epsilon_L}} \tag{10}$$

Transient response from the closed-loop frequency response.- The transient response for a step-input disturbance was obtained from the closed-loop response by Floyd's Method, an approximation method which is explained in detail in chapter 11, reference 1.

Briefly, the inverse transform $h(t)$ of $H(s)$, where $h(t)$ is the transient response to an impulse and $H(s)$ is a function of the complex operator s, is

$$h(t) = \frac{1}{2\pi j}\int_{c-j\infty}^{c+j\infty} H(s)e^{ts}ds \tag{11}$$

Under the conditions where s may be replaced by $j\omega$, an exact expression for the impulse response in terms of the real part of the closed-loop frequency response $H(j\omega)$ is

$$h(t) = \frac{2}{\pi}\int_{0}^{\infty} [\mathrm{Re}\ H(j\omega)\cos t\omega]\,d\omega \tag{12}$$

This integral may be approximated graphically. The procedure is to plot Re $H(j\omega)$ against ω and approximate the exact shape of the curve by a series of straight-line segments. This straight-line approximation defines a series of trapezoidal functions each of which can be evaluated by equation (12). The approximate value of $h(t)$ is then obtained by adding the resultant time functions.

For a series of trapezoidal functions such as is shown,

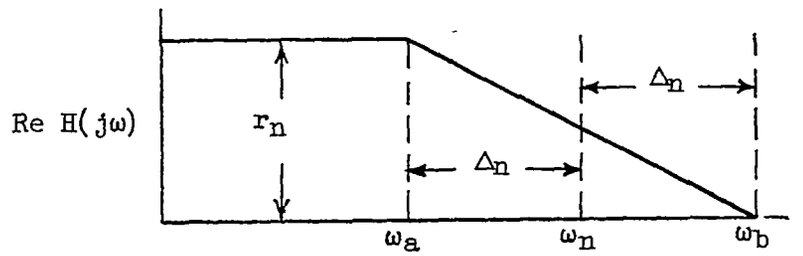

equation (12) can be evaluated as

$$h(t) = \sum_{n=1}^{k} \frac{2}{\pi} A_n \left(\frac{\sin \omega_n t}{\omega_n t}\right) \left(\frac{\sin \Delta \omega_n t}{\Delta_n t}\right)$$

where

k number of trapezoids used in approximating curve

A_n area of n^{th} trapezoid ($r_n \omega_n$)

ω_n $\frac{\omega_b + \omega_a}{2}$

Δ_n $\frac{\omega_b - \omega_a}{2}$

The step response may then be obtained by a graphical integration with respect to time of the impulse response.

TEST RESULTS AND CALCULATIONS

In this section are presented the test data and associated calculations required for analysis of system stability at the three test airspeeds of 85, 130, and 200 knots indicated at an altitude of 10,000 feet. The aircraft, servo system, and autopilot gearing are first considered individually. Hinge moment, required for gearing calculations, is also considered. The flight closed-loop frequency responses and their corresponding open-loop responses are then presented and compared with open- and closed-loop responses calculated from the component transfer functions. Finally, transient responses predicted from component frequency responses are compared with those measured in flight for the closed-loop system.

Aircraft Transfer Function

The dynamic characteristics of this component of the loop were obtained by analysis of flight-test data. Two types of flight maneuver, sine-wave forced oscillation and transient, were used as the source of aircraft-frequency-response data. The inputs were voltage disturbances of prescribed form introduced into the autopilot-aircraft loop (indicated by v_I in fig. 3). This technique avoided the considerable effort necessary to perform such forced oscillations in an unstabilized aircraft, necessitating, here, addition of a simple sine-wave voltage generator only. Transient inputs introduced in this fashion may be considered unusual to those who have not worked with stabilized aircraft. The actual elevator movement that produces the aircraft response does not assume the step function or pulse-type form, but is itself a damped oscillation. Thus, the work involved in analyzing the records is increased. The quantities measured for the study of this aircraft, which is stabilized in pitch, were pitch angle θ and elevator input angle δ_e. Sample forced-oscillation and transient-response records are presented in figure 4.

A straightforward method was utilized in extracting the aircraft frequency-response characteristics from the flight film records for the sine-wave oscillation tests. While the θ and δ_e records are not true sine waves, they were considered near enough, in most of the data, to warrant a simple analysis. The amplitude ratio was obtained by measurement of the amplitudes of the peaks and phase angle from the time differences between corresponding intercepts of the line drawn to equalize the half-cycle time intervals. Records not lending themselves to this procedure represented such a small portion of the data that they were disregarded.

The frequency response was obtained from transient data by use of equation (2) as discussed previously.

The final frequency-response characteristics are a combination of the results obtained from both types of flight tests. Sine-wave-oscillation data provide amplitude ratio values that repeat within ±3 percent for low values of frequency (0-0.3 cps) and to greater accuracy for values up to 1.6 cps. Sine-wave-oscillation phase angles were not considered to be of usable accuracy for the types of analyses that were attempted. Transient analyses provided consistent phase angles and amplitude ratios that varied within a maximum deviation of about 5 percent. The mean values of the transient-response amplitude ratios agreed well with those of the frequency response and the final amplitude-ratio curves (fig. 5(a)) are the faired average of both sine-wave oscillations and transient results. The final phase-angle characteristics (fig. 5(b)) are exclusively from transient data.

As a result of this investigation, it appears that, from considerations of flight time and practicable analysis procedures, the transient flight test is superior for obtaining frequency-response data for the airplane transfer function.

Autopilot Frequency Response

Extensive ground tests were made of the autopilot. These were performed with most of the equipment remaining in the fuselage to simulate the actual flight setup as closely as possible. The flight aerodynamic loads upon the elevator were simulated by torsional springs producing the required hinge moments. The autopilot frequency-response characteristics were determined for several values of displacement and rate-of-displacement feedback and input-signal amplitudes.

In order to choose input signals of a magnitude low enough to insure linear operation of the servo amplifier, it was first necessary to measure the static characteristic of the amplifier. This relation is shown in figure 6 where the output current is plotted as a function of the input voltage to the amplifier (servo-system error voltage). It can be seen that the relation is linear within about 10 percent over a range of ±0.35 volt about the voltage value required for zero unbalance current. This value of 0.35 volt is designated the nonlinearity level although it is evident that the system does not depart rapidly from linearity for another 0.1 volt or so.

Dynamic tests were conducted on the autopilot servo system coupled to the elevator control surface first using an electrical sinusoidal input signal. An amplitude ratio expressed as the ratio of the output motion at any frequency to that at zero frequency and a phase angle representing the number of degrees the output motion leads (considered plus) or lags (minus) the input signal were obtained. Tests were made for several values of simulated hinge moment but it was found that the dynamic response did not differ materially over the frequency range of primary interest, 0-1 cps. Hence the no-load responses were used for the analysis. Loading of the control surface does change the gearing, however, and this is discussed in the following two sections. The no-load, nondimensional frequency reponse A_p for the servo system is presented in figure 7(a) for a range of sensitivity settings, namely, 24, 33, 42, 52, and 63 percent. The magnitude of the input signal was ±0.115 volt, corresponding to about ±1/4° in pitch for the gyro constant used in the analysis. This magnitude was low enough to allow linear operation of the servo system throughout the frequency range.

To determine the response for rate signal in addition to displacement signal, tests were conducted with the gyros mounted on a sinusoidally oscillating table and their combined electrical output fed to the servo system. This nondimensional response is designated by the

factor $A_p(1+P_rA_r/k_g)$ and is shown in figure 7(b) for a sensitivity of 24 percent and rate settings of 0, 8, 20, and 31 percent. (These rate settings gave values for the ratio of rate to displacement signals, P_rA_r/k_g, of 0.83f, 2.07f, and 3.21f, respectively, up to a frequency of 1.2 cps. At higher frequencies the amplitude of A_r departed from its linear relationship with frequency.) The input magnitude was $\pm 1/4^o$ of table oscillation. With this input the responses with rate signal remained linear up to a little more than 1 cps. The responses for all rate signal values reached the nonlinearity level between 1 and 2 cps, the response at the lowest rate value being linear almost to 2 cps.

The response with rate signal was also calculated from the measured values of A_p, P_r, A_r, and k_g for the same conditions as above. The agreement with the response obtained from the oscillating table tests was very good. (See reference 3.) Hence, for a sensitivity of 42 percent, the rate responses were calculated rather than measured directly.

Hinge Moment

Ground tests of the autopilot installed in the airplane disclosed the fact that hinge moment directly affects the gearing factor k_p. With a flexible linkage connecting the servo actuator and control surface, as indicated in figure 3, the gearing will be decreased by addition of any load on the elevator due to stretching of the control cable. The hinge moment was determined from flight tests in order to eliminate it as a possible source of error in the predicted autopilot-aircraft responses.

The spring properties of the linkage between servo actuator and control surface were used to determine the hinge moments encountered in flight at the three test airspeeds. The linkage was calibrated on the ground and its spring constant determined. Both servo and surface positions were recorded on the ground under no load and in flight at the three airspeeds during the course of the frequency-response tests. Thus the change in the ratio of surface to servo deflections between ground and flight conditions was a measure of the hinge moment under dynamic tests. The average value of a number of runs for each indicated airspeed was as follows:

Knots	Foot-pounds per degree
85	3.0
130	10.0
200	21.6

Hinge moments were also estimated from wind-tunnel measurements on a similar airplane and were sufficiently close to the actual values as to have made no difference in the determination of the gearing factors.

Autopilot Gearing

The autopilot gearing factor k_p is defined as the static ratio of the control-surface deflection to pitch-attitude input to the autopilot. In this particular installation it is controlled by the sensitivity potentiometer but, as shown previously, it is also a function of hinge moment and, hence, airspeed.

The gearing factor was determined in several ways, all of which gave somewhat different results. The most complete determination was by means of introducing an electrical signal of several magnitudes, corresponding to various pitch angles, to the servo system with the airplane on the ground and measuring the control-surface deflection. This was done for no load on the surface and at three values of simulated hinge-moment load, 2, 8, and 20 foot-pounds per degree, corresponding roughly to the test airspeeds of 85, 130, and 200 knots. A range of sensitivity settings was also covered for each load. To obtain the corresponding pitch angle, the vertical gyro was calibrated by rotating it 0.1° at a time and measuring the output voltage. Thus the gyro constant k_g was found to be 0.51 volt per degree. The gearing is then the product of this constant and the values of surface deflection per volt input to the servo system. To obtain a linear relation, the reciprocal of the gearing $1/k_p$ is plotted in figure 8 against sensitivity for the various loads. The data are replotted in figure 9 to show the reciprocal gearing $1/k_p$ plotted against load for varying sensitivities. From this figure the gearings corresponding to the test airspeeds were obtained and used in the analysis presented in this report.

The gearing for the no-load case was determined also by measuring the control-surface deflection for various attitude settings of the vertical gyro which was connected to the rest of the autopilot in the normal manner as in figure 3. In another test the gyro was mounted on an oscillating table and oscillated sinusoidally at low frequencies (between 0.1 and 0.2 cps) at several amplitudes, and the control-surface deflections were recorded. The values obtained from these two types of tests were not in good agreement with each other or those obtained previously. Furthermore, it was observed that the values seemed to depend on the servo displacement, being considerably less for small displacements. This is the type of behavior typifying systems containing nonlinearity caused by play or backlash, and indicates one probable cause for discrepancies between flight and predicted responses.

This effect could not be resolved without considerably more investigation than was justified in this case. The values obtained from figure 9 gave predicted autopilot-aircraft open-loop responses which, on the whole, most nearly matched those obtained from flight and therefore were used in the analysis.

The Autopilot-Aircraft Combination

Open-loop, closed-loop, and transient responses for the autopilot-aircraft combination were predicted from tests of the components and also obtained experimentally in flight over a wide range of sensitivity and rate-of-pitch feedback conditions for each of the three airspeeds. The conditions tabulated were selected for presentation in this report not only because they include representative sensitivity and rate settings, but also because they illustrate the effect of changes in airspeed, sensitivity, and rate upon the system performance.

Airspeed (knots)	Sensitivity (percent)	Rate (percent)	Figure (number)
85	42	0	10(a)
130	42	0	10(b)
200	42	0	10(c)
130	63	0	10(d)
130	24	8	10(e)
130	24	31	10(f)
130	42	8	10(g)
130	42	20	10(h)
130	42	31	10(i)

The open-loop, closed-loop, and transient responses each provide information of a vital, although different, nature about the stability and performance of the autopilot-aircraft combination and is plotted upon the same page for each of the above conditions. (See figs. 10(a) to 10(i).) In each figure the predicted response is compared with the response measured in flight or one derived therefrom. The methods of calculation have been presented in the foregoing sections and a sample calculation for each type is given in the appendix.

All calculations were based on the assumption of linear operation of all components. This assumption holds throughout the frequency range for very small inputs only. For the flight tests an input magnitude equivalent to $\pm 1/2^{\circ}$ was used. This value was not low enough to insure linear operation all the time, but it was as small as practicable from the standpoint of accuracy of measurements. It is also believed to be a reasonable value, one that might likely be encountered in flight as an external disturbance. The error voltage for the closed-loop combination was calculated in each case.

The open-loop frequency response is shown at the top of each page plotted on polar coordinates representing amplitude and phase angle. This form is commonly known as a Nyquist diagram. The nearness of the curve to the 1, -180° point is an indication of the relative stability of the system. The frequency is also given for each point shown on the curve. The predicted curve, shown by a broken line, was calculated from measurements of the individual components of the autopilot-aircraft loop. The solid curve, in this case, was calculated from the closed-loop frequency response of the combination measured in flight.

The closed-loop frequency-response amplitude and phase-angle curves are shown on the middle of each page plotted against frequency. The predicted curve was calculated from the predicted open-loop response. The solid curve was obtained directly from flight measurements of the closed-loop frequency response.

The transient responses for a unit step input are shown at the bottom of each page. The predicted curve was obtained from the predicted closed-loop frequency response by the approximation method previously discussed. The solid curve was obtained from flight measurements of the transient response to a step voltage input to the autopilot equivalent to $1/2^{\circ}$ of pitch.

DISCUSSION

The three major aspects of the analysis to be discussed are the agreement between experimental and predicted results, the effect of displacement and rate of displacement feedback, and the effect of airspeed.

Of primary interest is the degree of agreement between the flight-measured responses of the autopilot-aircraft combination and those predicted from the component transfer functions. To serve as a basis of comparison, the important information which can be obtained from the response plots can be summarized as follows: For the open-loop plot, the values of phase margin and gain margin specify the performance to a certain degree, the former usually being the most critical with respect to stability. On the closed-loop frequency-response plot, the peak-amplitude ratio and the frequency at which it occurs are significant points. For the transient response there are several characteristics of interest, such as the response time (time to first reach the desired value), peak overshoot, cycles to damp to a certain fraction of the final displacement, period or frequency of the oscillations, etc.

In general, it was found that agreement between measured and predicted responses was satisfactory for most cases, but was unsatisfactory when rate signal was used with a displacement setting that results in a nearly unstable response without rate signal.

The responses for the condition of zero rate and various sensitivities and airspeeds are presented in figures 10(a), (b), (c), and (d). It can be seen that the agreement between measured and predicted values is very good for a sensitivity of 42 percent at the three airspeeds. The comparison at 200 knots (fig. 10(c)) is an example of the best agreement obtained in the analysis and is considered to be well within experimental error. For each of these cases at 42 percent sensitivity, phase margins agree within about 5°, and gain margins, peak amplitude ratios, and resonant frequencies are within a few percent. However, it may be noticed in all these figures that the transient-response agreement is not as good as that for the frequency responses. The discrepancy is actually between the flight sinusoidal and transient data since the transient peak obtained in flight is higher than would be obtained from an analysis of the corresponding sinusoidal response. A possible cause of this difference may be drift of the vertical gyro over the duration of the transient which may result in errors when normalizing the transient-response plot about the final steady-state value.

For a sensitivity of 63 percent (fig. 10(d)), there is a discrepancy between the frequency-response curves which is greatest at the low frequencies on the open-loop polar diagram. This difference may partially be explained by backlash in the elevator-linkage system. As the control gearing is reduced (increased servo sensitivity), the control-surface deflection becomes smaller, being smallest at low frequencies where the airplane is closely following the pitch-input signal. Hence, the backlash region becomes a greater percentage of the total surface deflection. Thus, the control gearing would be effectively reduced at the lower frequencies where surface deflection is smallest. An increase in gearing applied to the flight open-loop response curve would bring it into agreement with the predicted curve with the exception that the frequencies would not correspond.

For high values of gearing the agreement was considered excellent. Although a figure is not presented for a sensitivity of 24 percent, the predicted closed-loop response had an amplitude ratio peak of about 12 which indicates a condition dangerously close to instability. The flight response was just about at the point of neutral stability. In response to a transient, the combination would oscillate sometimes with increasing amplitude of oscillation and sometimes with a very gradual decay in amplitude of oscillations. An experimental frequency response could not be obtained because of the tendency to break into instability.

The responses with rate-of-displacement feedback in addition to displacement feedback are presented in figures 10(e) through 10(i). The agreement at a sensitivity of 24 percent when there is rate feedback (figs. 10(e) and (f)) is seen to be poor; whereas the agreement at a sensitivity of 42 percent (a lower gearing) with rate feedback (figs. 10(g), (h), and (i)) is good, particularly with respect to phase margin. As previously mentioned, the sensitivity setting of 24 percent is one which results in a neutrally stable response without the addition

of rate. The nearness of the over-all system to instability at this sensitivity for the cases with rate feedback is discussed in more detail later and provides a clue to the discrepancies. The system behavior becomes quite critical under these conditions and small changes in component values may result in large changes in the system response. It should be noted, however, that the curves shown in figure 10(f) represent about the best transient response obtained in flight. The error voltage was calculated in each of the above cases and was found to cause saturation only at a sensitivity of 24 percent at frequencies close to the resonant frequency.

The difficulty in determining the values of gearing has been discussed previously and was attributed to the nonlinear characteristics of the linkage system. The possibilities of both amplitude and phase of elevator deflection being distorted relative to servo displacement and to forcing frequency may account for some of the discrepancies encountered in the predicted results.

A second major point of interest in the results is the effect on the autopilot-aircraft response of changes in displacement and rate of displacement feedback. As was mentioned previously, a sensitivity of 24 percent with zero rate signal resulted in a highly oscillatory response which frequently broke into instability. Figures 10(b) and (d) show the effect of increasing the sensitivity (decreasing the gearing). As is to be expected, the lower the gearing, the higher the damping but the longer the response time. Flight tests bore out the prediction that the response would be very slow if the gearing were reduced to the point of giving satisfactory damping, say a value of 0.7 of the critical damping.

The foregoing discussion points out the need of additional stabilization factors and, hence, rate of displacement signal was added to the feedback. It can be seen from a consideration of the transient responses in figures 10(e) and (f) that as the rate signal is increased the damping is improved at no expense in response time. A sensitivity of 24 percent and a rate of 31 percent (fig. 10(f)) provided the fastest response with the least amount of overshoot of any of the possible settings of the autopilot.

It is important to note, however, that consideration must be given other factors in choosing the most desirable response based on the criteria given in the foregoing paragraph. A response obtained with the aid of an autopilot that is considerably better than the response of the aircraft alone generally requires a large amount of total control-surface motion. This may be objectionable from the standpoint of servo energy required or excessive wear on the control system.

An equally or more important consideration is the nearness of the system to instability. When rate or other derivative types of feedback are used, this nearness is not shown by the closed-loop frequency or

transient response θ/θ_I since the output and input are not determined at the same point in the loop. The relative system stability is obtained basically from an examination of the open-loop response. A qualitative idea can also be obtained from the closed-loop response $(\theta+\theta_r)/\theta_I$ (with reference to the diagram on p. 11) which may be rewritten as $\theta(1+P_rA_r/k_g)/\theta_I$. From this it can be seen that the desired θ/θ_I response must be multiplied by the feed-back factor $(1+P_rA_r/k_g)$ to check on the system stability. A limit then exists on the amount of rate feedback that can be used to improve the θ/θ_I response. The real importance of this consideration is that for systems adjusted to obtain the optimum θ/θ_I response small changes in system characteristics might be sufficient in extreme cases to change the response from highly satisfactory to highly unsatisfactory.

By reference to the experimental results in figures 10(e) and (f) and by consideration of the neutrally stable response for this sensitivity setting (24 percent) at zero rate, it is seen that as rate signal is progressively increased the flight transient response is improved but the corresponding open-loop response first becomes more stable and then moves closer to instability. Further increase of rate signal during flight tests resulted in actual instability of the combination as would be expected. This same trend can also be observed in figures 10(b), (g), (h), and (i).

A third point of interest in the results of the analysis is the change in response with airspeed for a given sensitivity setting. This is shown in figures 10(a), (b), and (c). Examination of these responses indicates that they are essentially the same for all airspeeds. The phase margins vary from 20° to 30°, gain margins from 2-1/2 to 5, and peak amplitude ratios from 2 to 2-1/2. This close agreement for different airspeeds may appear surprising until it is recalled that the gearing is unintentionally altered in the favorable direction by hinge moment due to the elasticity of the control linkage. It appears that the spring constant is such that the change in gearing compensates for the change in the aircraft response with airspeed.

To illustrate what would have happened to the combination response if the gearing had not changed with airspeed, consider the values of the reciprocal gearing $1/k_p$ obtained from figure 9 for a sensitivity of 42 percent at 85 and 200 knots which are 0.92 and 1.97, respectively. This represents a change of approximately 2 to 1. Hence, if the system were adjusted to give the response at 85 knots as shown in figure 10(a), the open-loop response for 200 knots (fig. 10(c)) would be increased radially by a factor of 2 to 1. The 0.8-cps point would then be moved out to the unity-gain circle resulting in a phase margin of only 15°. The gain margin would be reduced to about 1.6. The resulting transient response would then be too oscillatory and the system dangerously close to instability. The same would be true if the system were adjusted at 200 knots and then flown at an appreciably higher speed. In this

particular installation, the flexibility of the linkage system probably saved the airplane from destruction in automatically controlled high-speed dives.

CONCLUSIONS

1. If the optimum response (not merely a conservatively stable response) for an autopilot-aircraft combination is to be predicted by linear analysis procedures, assurance must be obtained that the component performances are actually linear or very close to it. Predicted responses may deviate considerably from flight results due to a combination of several small nonlinearities such as in control linkage lost motion, amplifier saturation, etc.

2. The over-all-system, open-loop response must be inspected for the nearness of the system to instability. Even though the transient response of particular interest appears well damped, the system may be nearly unstable; thus a slight change in component performance might result in instability.

3. The effects of airspeed on autopilot-aircraft stability may be compensated for over the range in which the hinge moment is roughly proportional to elevator effectiveness by means of a simple spring mechanically linking the control surface to the servo actuator. Dynamic effects of the spring must, of course, be considered in the design.

Ames Aeronautical Laboratory
National Advisory Committee for Aeronautics
Moffett Field, Calif., Sept. 20, 1951

APPENDIX

ILLUSTRATIVE EXAMPLE OF CALCULATIONS

Airspeed 130 knots, sensitivity 24 percent, and rate 8 percent (fig. 10(e)) was selected as the condition to illustrate the calculations necessary for a comparison of predicted and flight closed-loop, open-loop, and transient responses. This setting was chosen because, since rate feedback is present, it illustrates in the most general fashion the calculations required.

The open-loop and closed-loop responses are calculated in this example only for a single frequency ($f = 0.8$ cps) since the procedure will be identical throughout the frequency band. However, due to the nature of the method, a complete transient calculation is carried out.

During flight, records were obtained of the pitch response of the stabilized airplane to sinusoidal and step-inputs of known magnitude. The closed-loop flight response, θ/θ_I, was obtained from the record of the attitude of the airplane θ in response to the sinusoidal inputs:

$$\frac{\theta}{\theta_I} = \left(\frac{\theta}{v_I}\right)\left(\frac{v_I}{\theta_I}\right) = \theta\,\frac{k_g}{v_I}$$

At $f = 0.8$ cps,

$$\theta = 0.575\ \underline{/-197^\circ}$$

$$v_I = 0.25 \text{ volts}$$

$$k_g = 0.51 \text{ volts/ degree}$$

Substituting these values in the above equation gives

$$\frac{\theta}{\theta_I} = 1.17\ \underline{/-197^\circ}$$

The experimental open-loop response A_L is computed from θ/θ_I by means of equation (5):

$$A_L = \frac{\left(\frac{\theta}{\theta_I}\right)\left(1+\frac{P_rA_r}{k_g}\right)}{1-\left(\frac{\theta}{\theta_I}\right)\left(1+\frac{P_rA_r}{k_g}\right)}$$

where the feed-back factor $(1+P_rA_r/k_g)$ can be evaluated by equation (6) from the rate and no-rate servo responses (fig. 7(b)), where

$$\left(1+\frac{P_rA_r}{k_g}\right) = \frac{\left[A_p\left(1+\frac{P_rA_r}{k_g}\right)\right]_{measured}}{A_p}$$

At f = 0.8 cps,

$$\left[A_p\left(1+\frac{P_rA_r}{k_g}\right)\right]_{measured} = 1.68 \angle 7^\circ \quad \text{(from fig. 7(b))}$$

$$A_p = 1.10 \angle -31^\circ \quad \text{(from fig. 7(b))}$$

therefore

$$\left(1+\frac{P_rA_r}{k_g}\right) = \frac{1.68 \angle 7^\circ}{1.10 \angle -31^\circ} = 1.53 \angle 38^\circ$$

and

$$A_L = \frac{(1.17 \angle -197^\circ)(1.53 \angle 38^\circ)}{1-(1.17^\circ \angle -197^\circ)(1.53 \angle 38^\circ)} = 0.66 \angle -173^\circ$$

The predicted open-loop response was obtained by multiplying the dimensionless autopilot-with-rate response, the aircraft response, and the proper gearing (equation (7)):

$$A_L = k_pA_p\left(1+\frac{P_rA_r}{k_g}\right)A_\theta$$

at $f = 0.8$ cps,

$$A_\theta = 0.39 \angle -157^\circ \text{ (from fig. 5)}$$

$$k_p = 1.52 \text{ (from fig. 9)}$$

$$A_p \left(1+ \frac{P_r A_r}{k_g}\right) = 1.68 \angle 7.0^\circ \text{ (from fig. 7(b))}$$

$$A_L = 1.52\ (1.68 \angle 7.0^\circ)(0.39 \angle -157^\circ) = 0.98 \angle -150^\circ$$

The predicted closed-loop response in terms of the open-loop response and the rate factor, equation (9), is:

$$\frac{\theta}{\theta_I} = \frac{A_L}{\left(1+ \frac{P_r A_r}{k_g}\right)\left(1+A_L\right)} =$$

$$\frac{0.98 \angle -150^\circ}{(1.53 \angle 38^\circ)(1+0.98 \angle -150^\circ)} = 1.24 \angle -114^\circ$$

The error voltage of the autopilot-airframe combination was calculated using the closed-loop no-rate servo response and the open-loop flight response by means of equation (10).

$$|v_{ec}| = v_I \sqrt{\frac{1+R^2-2R \cos \epsilon_f}{1+|A_L|^2+2|A_L| \cos \epsilon_L}}$$

at $f = 0.8$ cps,

$$R \angle \epsilon_f = 1.1 \angle -31^\circ \text{ (from fig. 7)}$$

$$A_L = 0.67 \angle -167^\circ$$

$$v_{ec} = 0.25 \sqrt{\frac{1+1.21 - 1.89}{1+0.45 - 1.31}} = 0.38$$

The predicted transient response was obtained by Floyd's Method which is outlined on page 14. For airspeed 130 knots, rate 8 percent, sensitivity 24 percent, Re $H(j\omega)$, which in this case is Re $\theta/\theta_I(j\omega)$, was plotted as a function of frequency f and the resultant curve was approximated by straight-line segments as shown in figure 11. The values of r, f, and the corresponding ω are tabulated as follows:

$r_o = 1.00$	$f_a = 0.34$	$\omega_a = 2.14$
$r_1 = .75$	$f_b = .53$	$\omega_b = 3.34$
$r_2 = .35$	$f_c = .64$	$\omega_c = 4.03$
$r_3 = .60$	$f_d = .83$	$\omega_d = 5.22$
$r_4 = .95$	$f_e = 1.004$	$\omega_e = 6.30$
	$f_f = 130$	$\omega_f = 8.17$
	$f_g = 1.75$	$\omega_g = 10.10$

Since all of the component trapezoids must be measured from the origin, Re $H(j\omega)$ was approximated by the sum of the trapezoids (with proper sign affixed) as shown in figure 12. Upon evaluation

$$h(t) = \frac{2}{\pi} \sum_{n=1}^{7} A_n \left(\frac{\sin \omega_n t}{\omega_n t}\right) \left(\frac{\sin \Delta_n t}{\Delta_n t}\right)$$

yielded the impulse response shown in figure 13, which, upon integration, yielded the step response shown in figure 10(e).

REFERENCES

1. Brown, Gordon S., and Campbell, Donald P.: Principles of Servomechanisms. John Wiley and Sons, Inc., N.Y., 1948.

2. Jones, Arthur L., and Briggs, Benjamin R.: A Survey of Stability Analysis Techniques for Automatically Controlled Aircraft. NACA TN 2275, 1951.

3. Smaus, Louis H., and Stewart, Elwood C.: Practical Methods of Calculation Involved in the Experimental Study of an Autopilot and the Autopilot-Aircraft Combination. NACA TN 2373, 1951.

4. Greenberg, Harry: A Survey of Methods for Determining Stability Parameters of an Airplane From Dynamic Flight Measurements. NACA TN 2340, 1951.

5. LaVerne, Melvin E., and Boksenbom, Aaron S.: Frequency Response of Linear Systems from Transient Data. NACA Rep. 977, 1950. (Formerly NACA TN 1935)

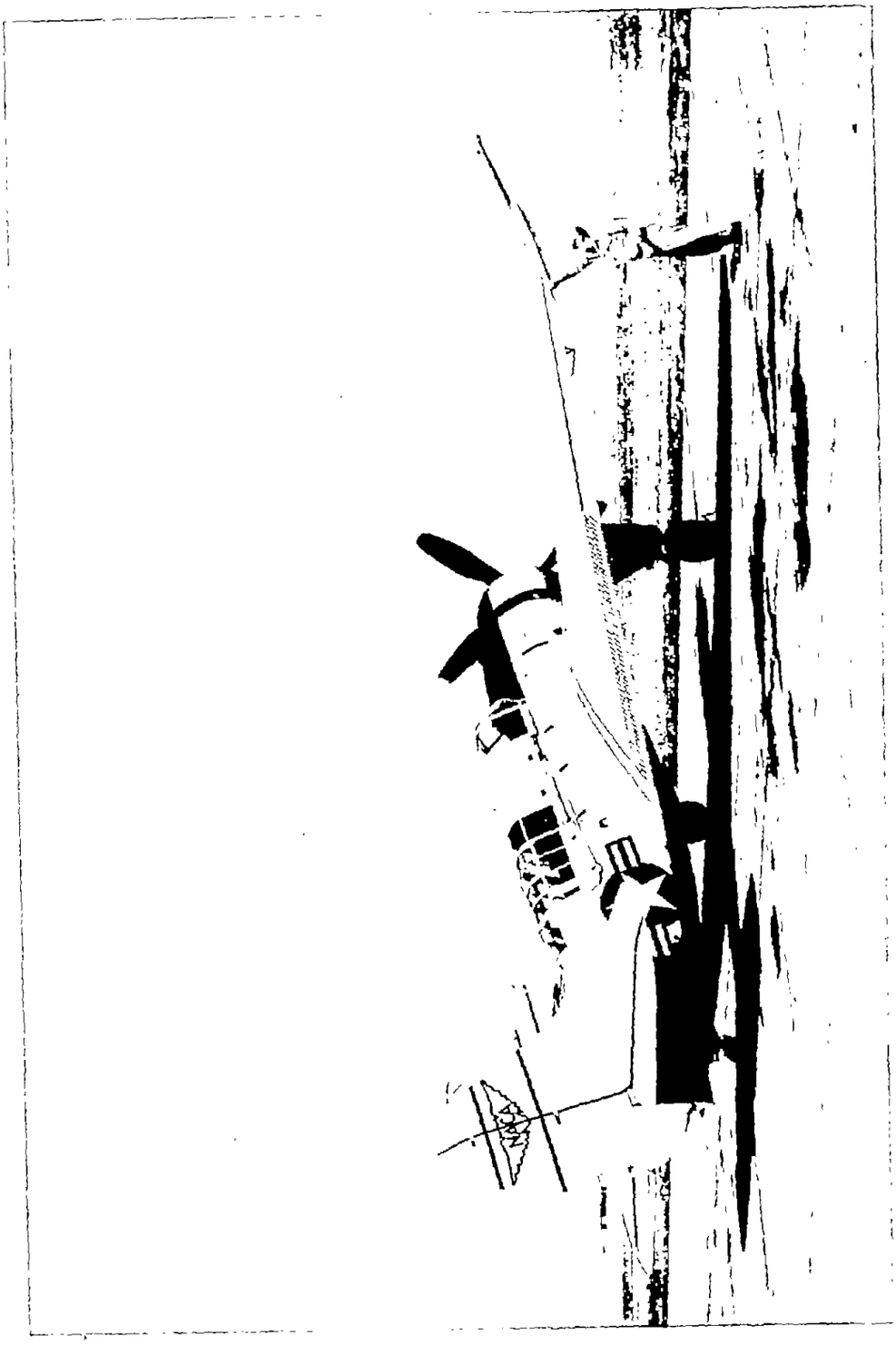

Figure 1.- Photograph of the airplane.

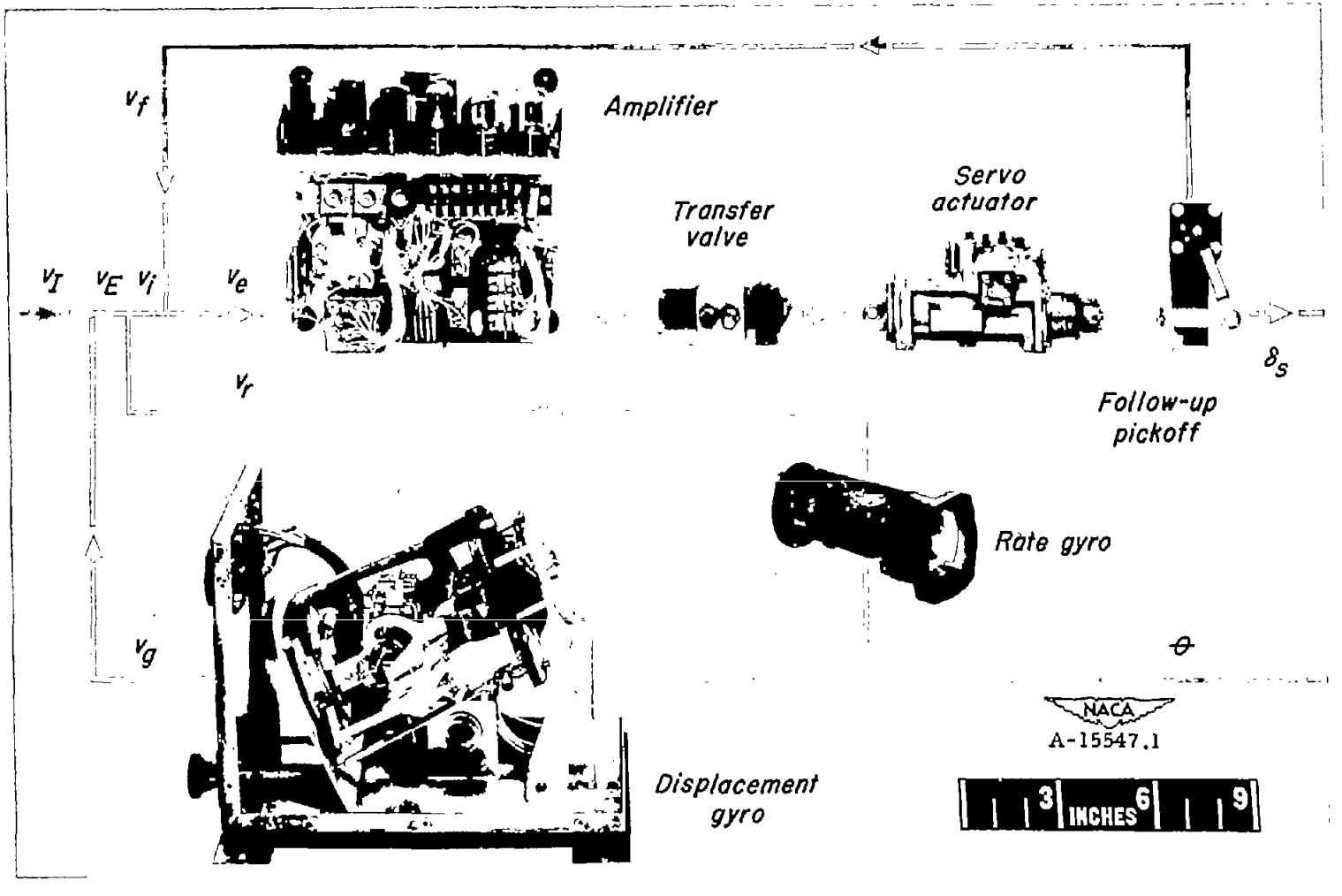

Figure 2.– Schematic photograph of the autopilot components.

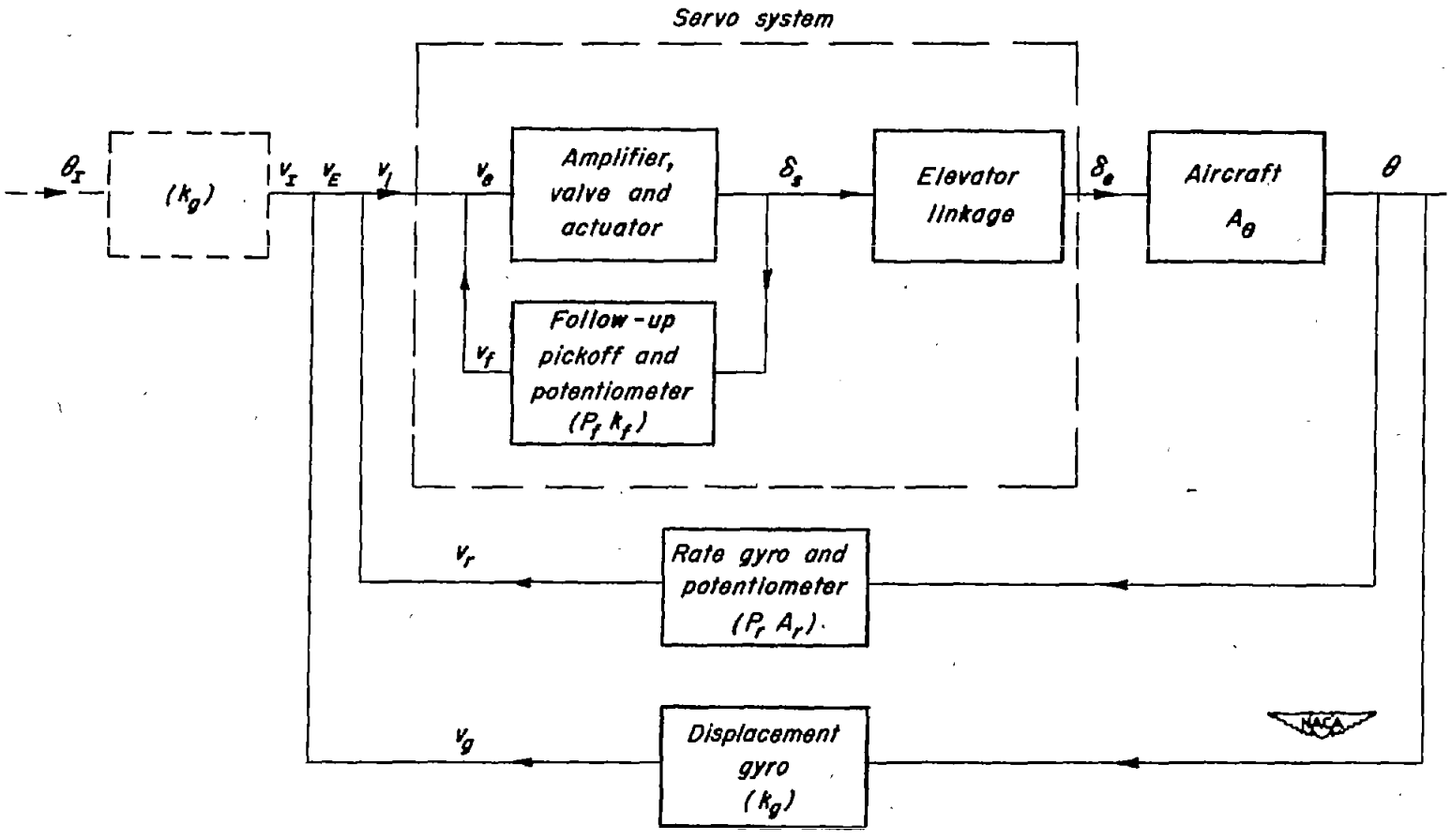

Figure 3.- Block diagram of autopilot-aircraft loop.

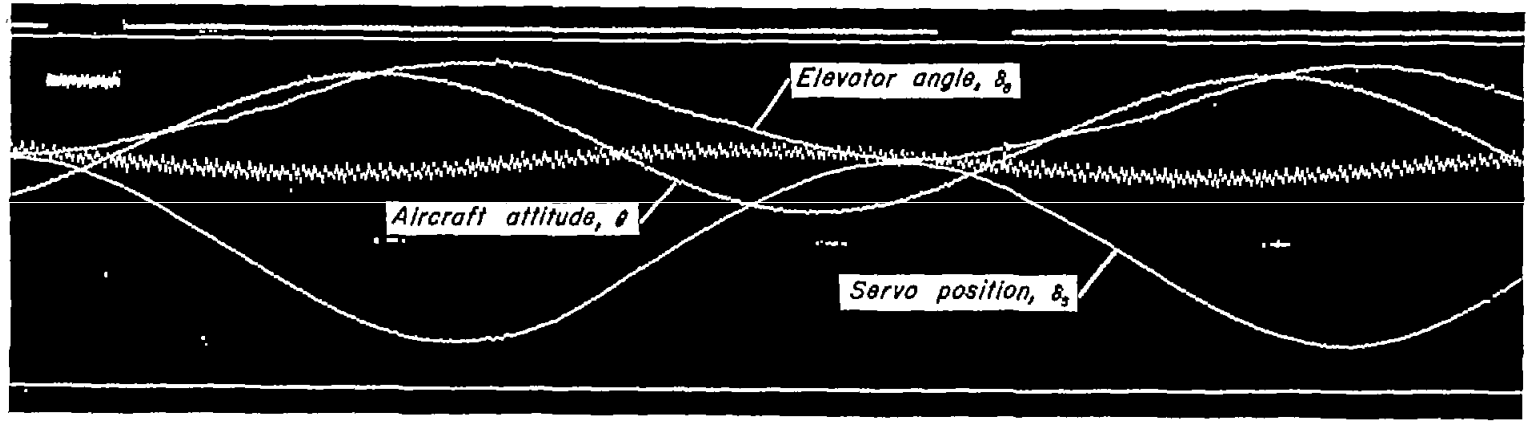

(a) Forced oscillation response.

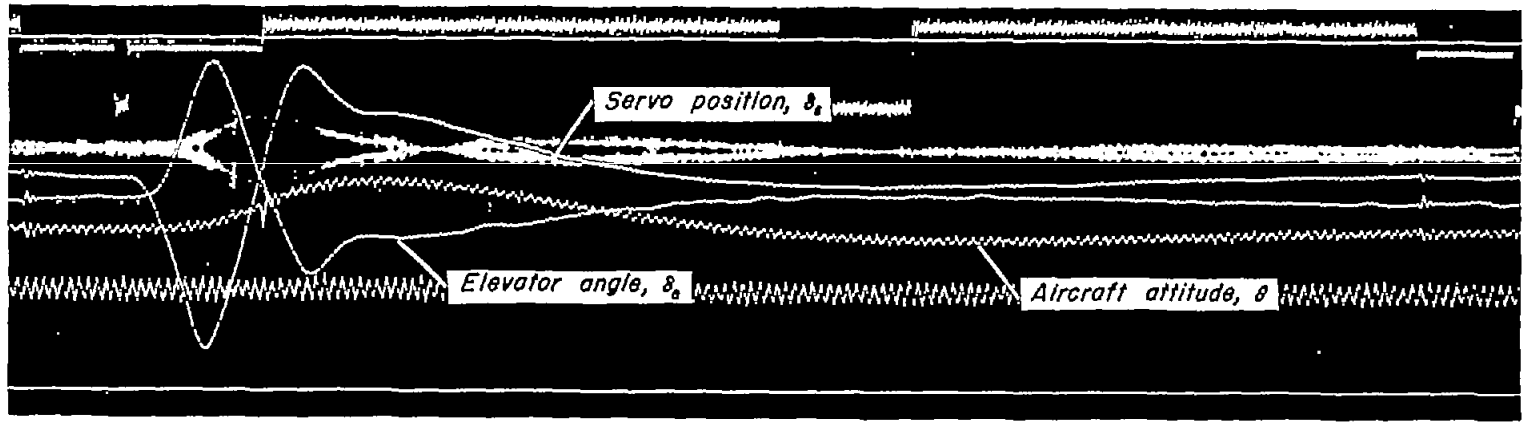

(b) Transient response to pulse voltage disturbance.

Figure 4.- Sample oscillograph records obtained during longitudinal dynamic stability tests of the stabilized test airplane.

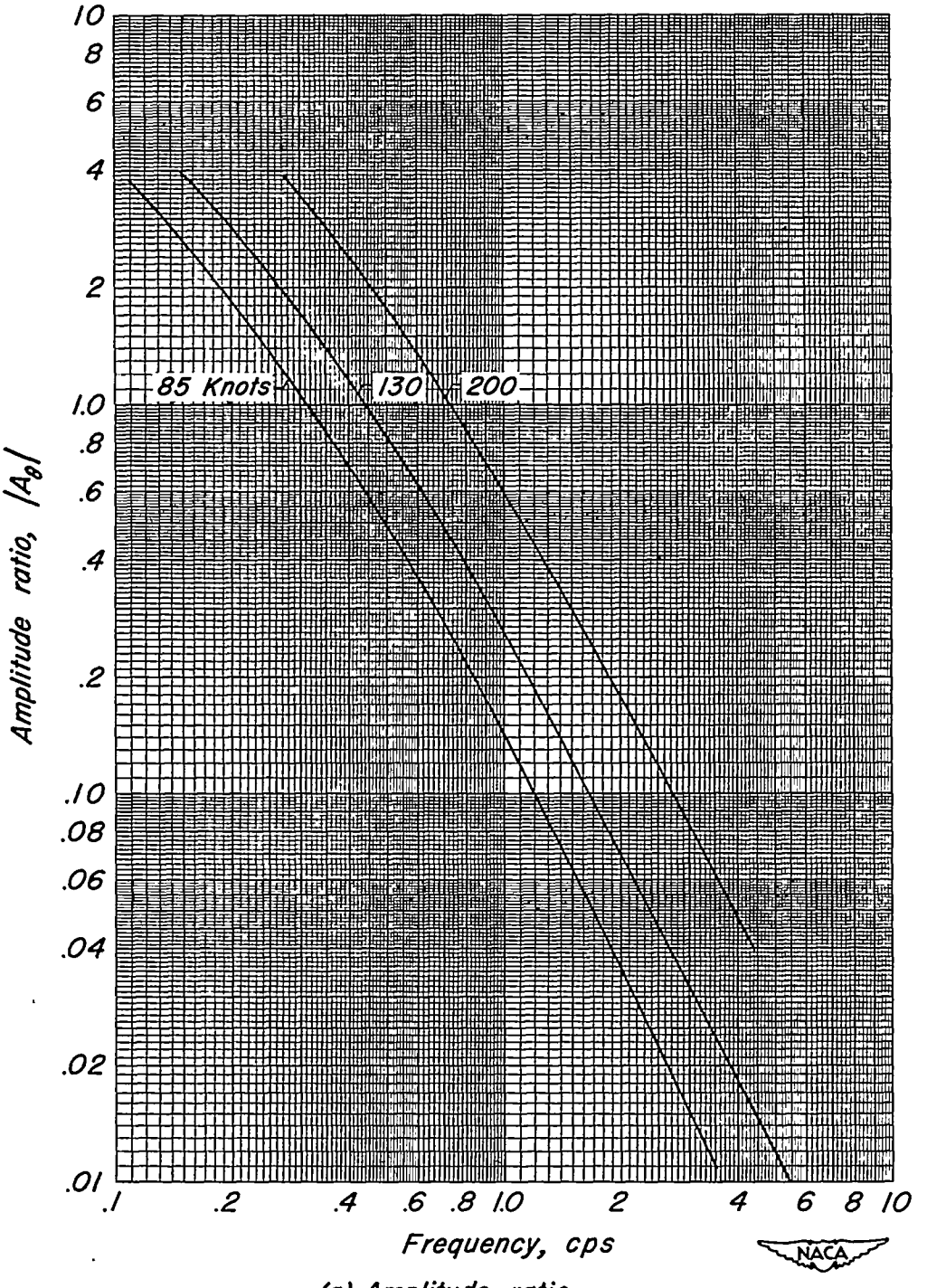

(a) Amplitude ratio.

Figure 5.- Airplane frequency response in pitch.

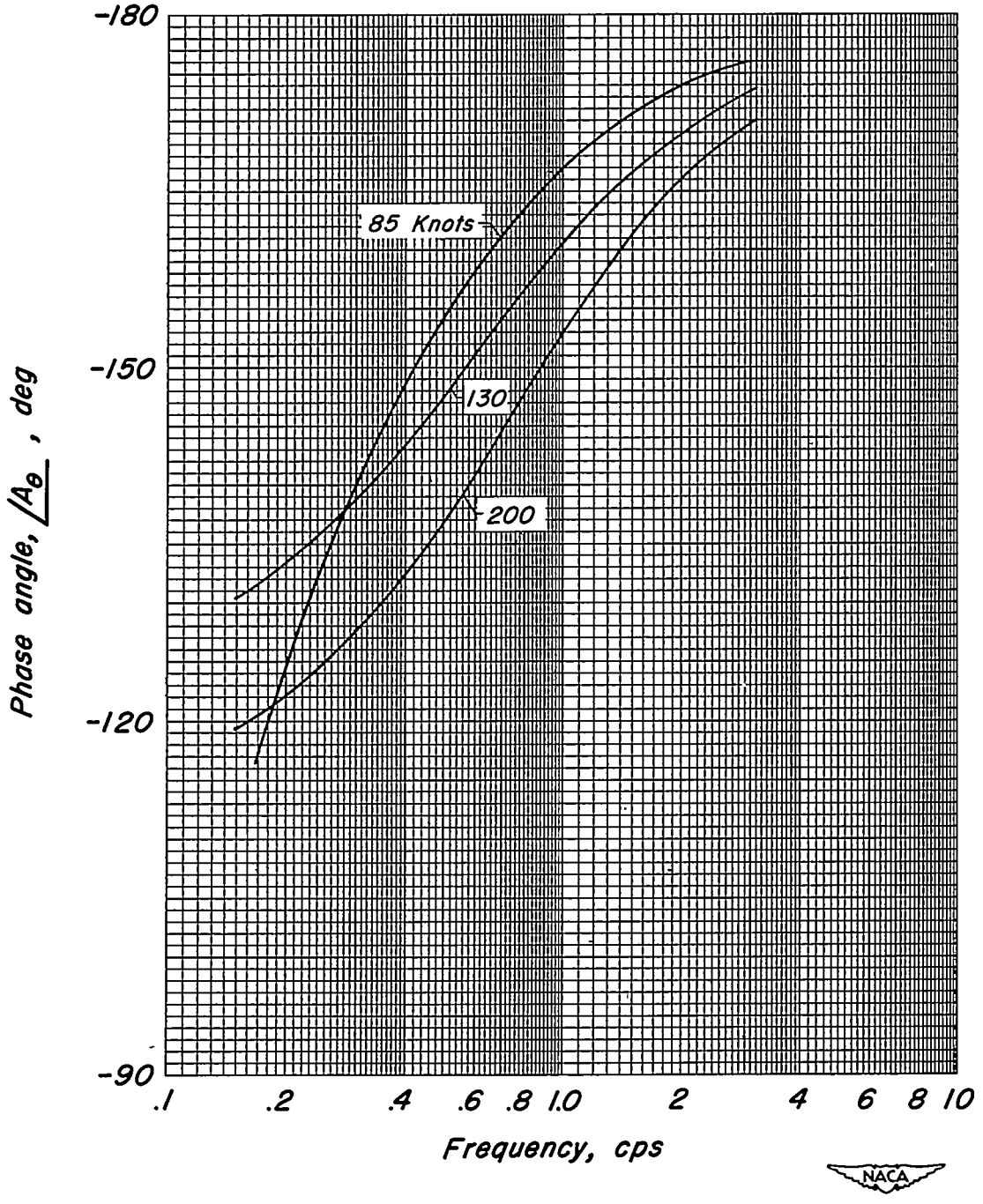

(b) Phase angle.

Figure 5.- Concluded.

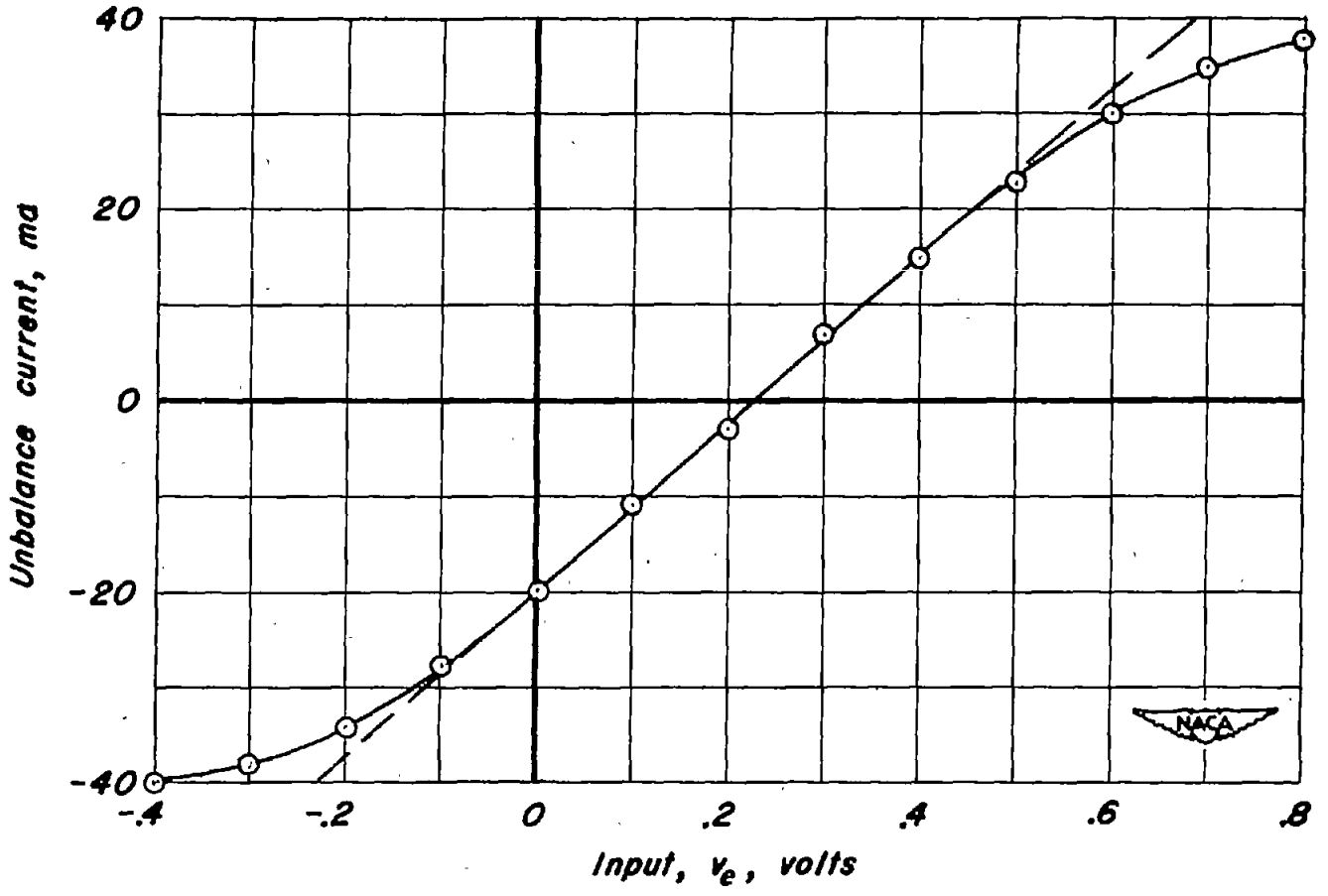

Figure 6.- Servo-amplifier gain characteristics.

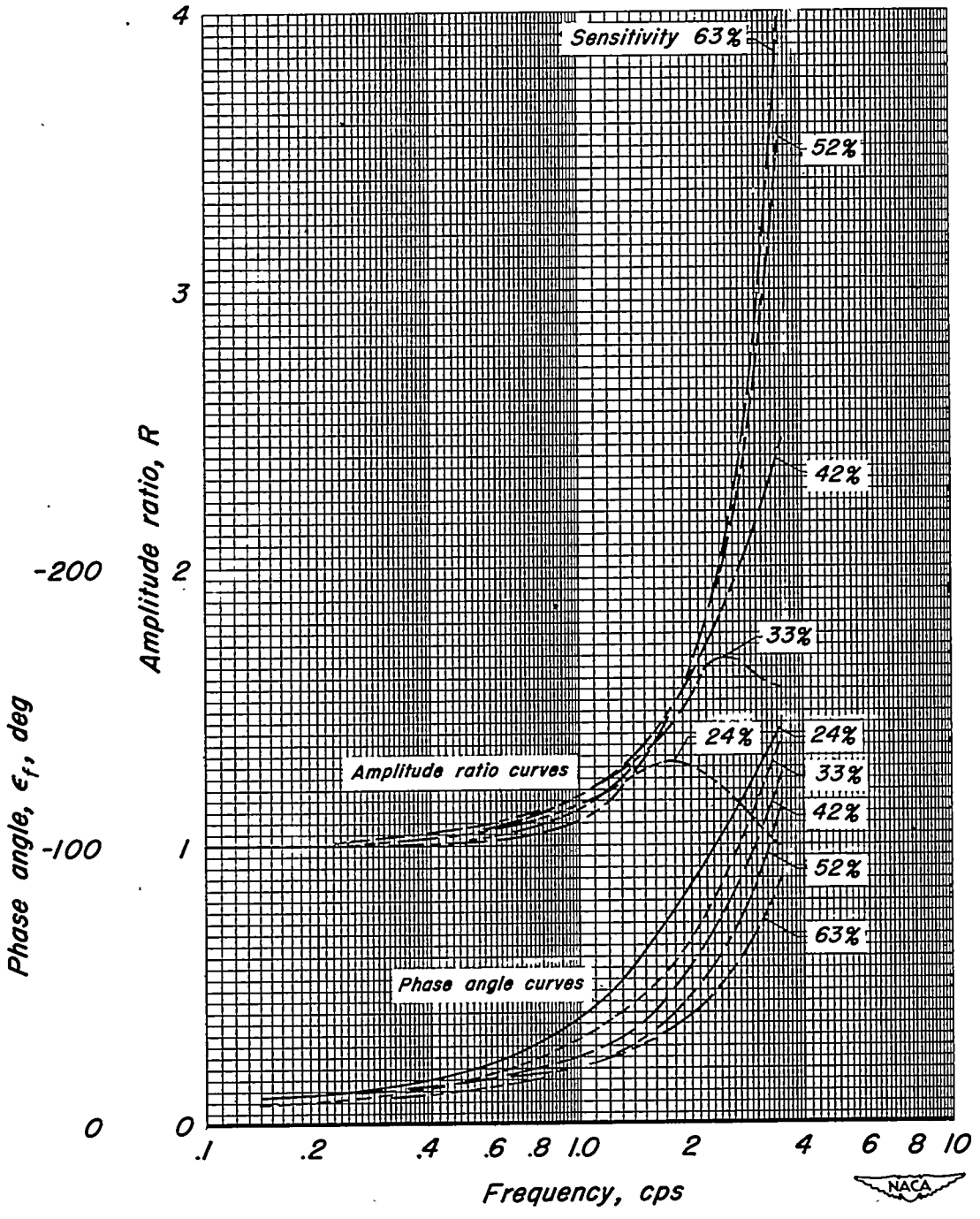

(a) Rate 0, various sensitivities, ±0.115 volt (≈0.25°) input.

Figure 7.- Autopilot response.

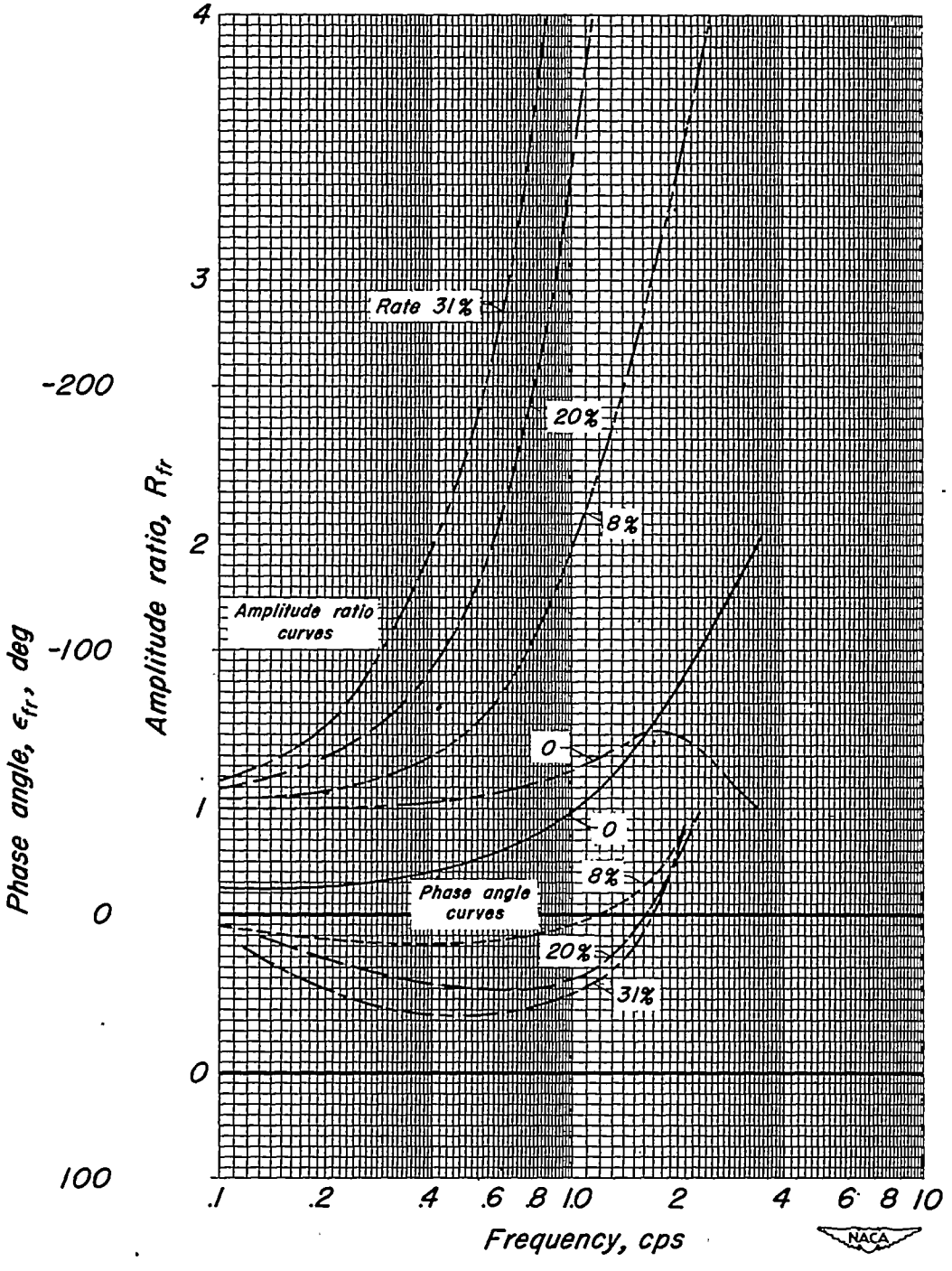

(b) Sensitivity 24 percent, various rates, ±0.25° input.

Figure 7.- Concluded.

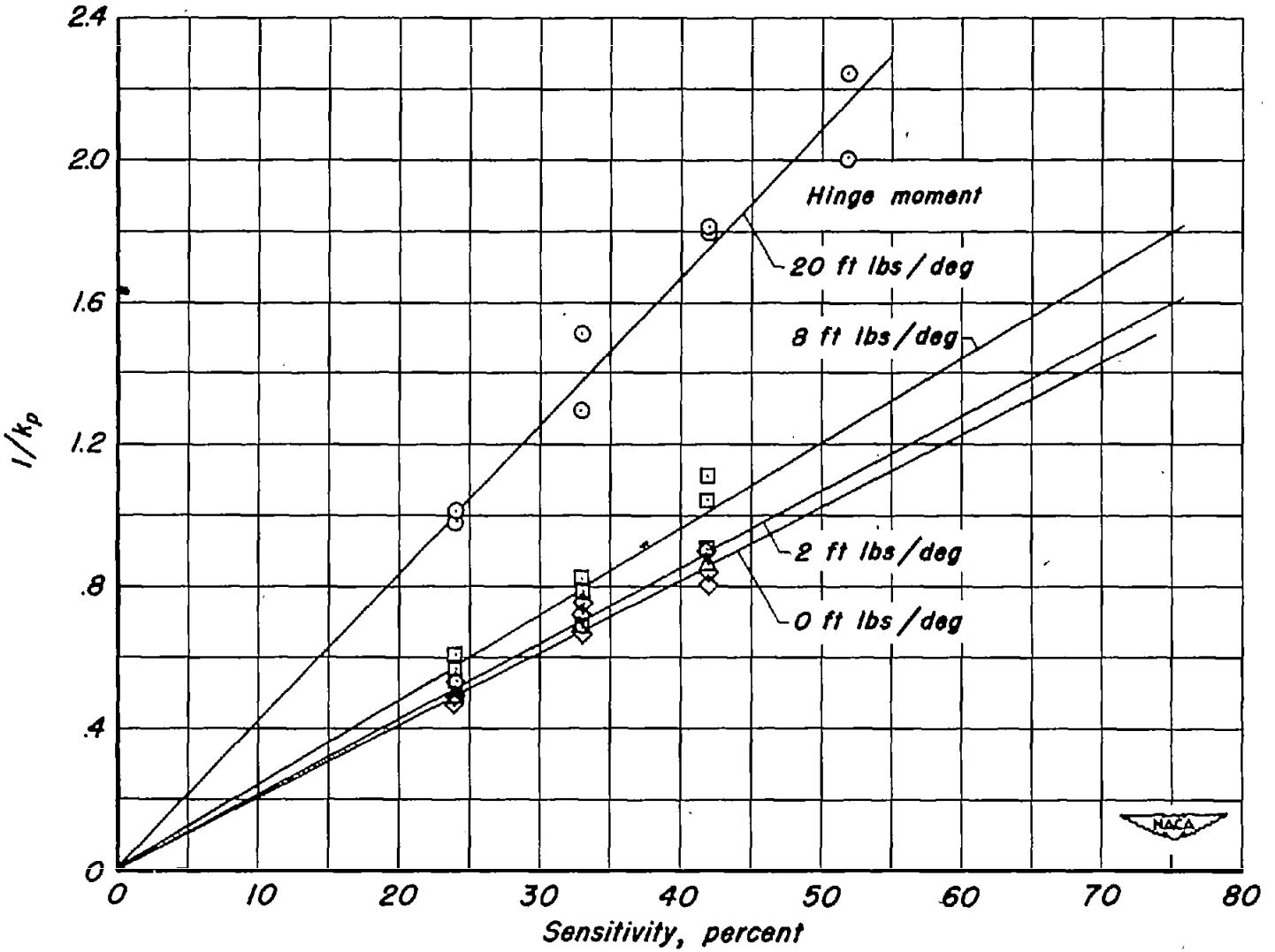

Figure 8.- Reciprocal gearing, $1/k_p$, versus sensitivity for various hinge moments.

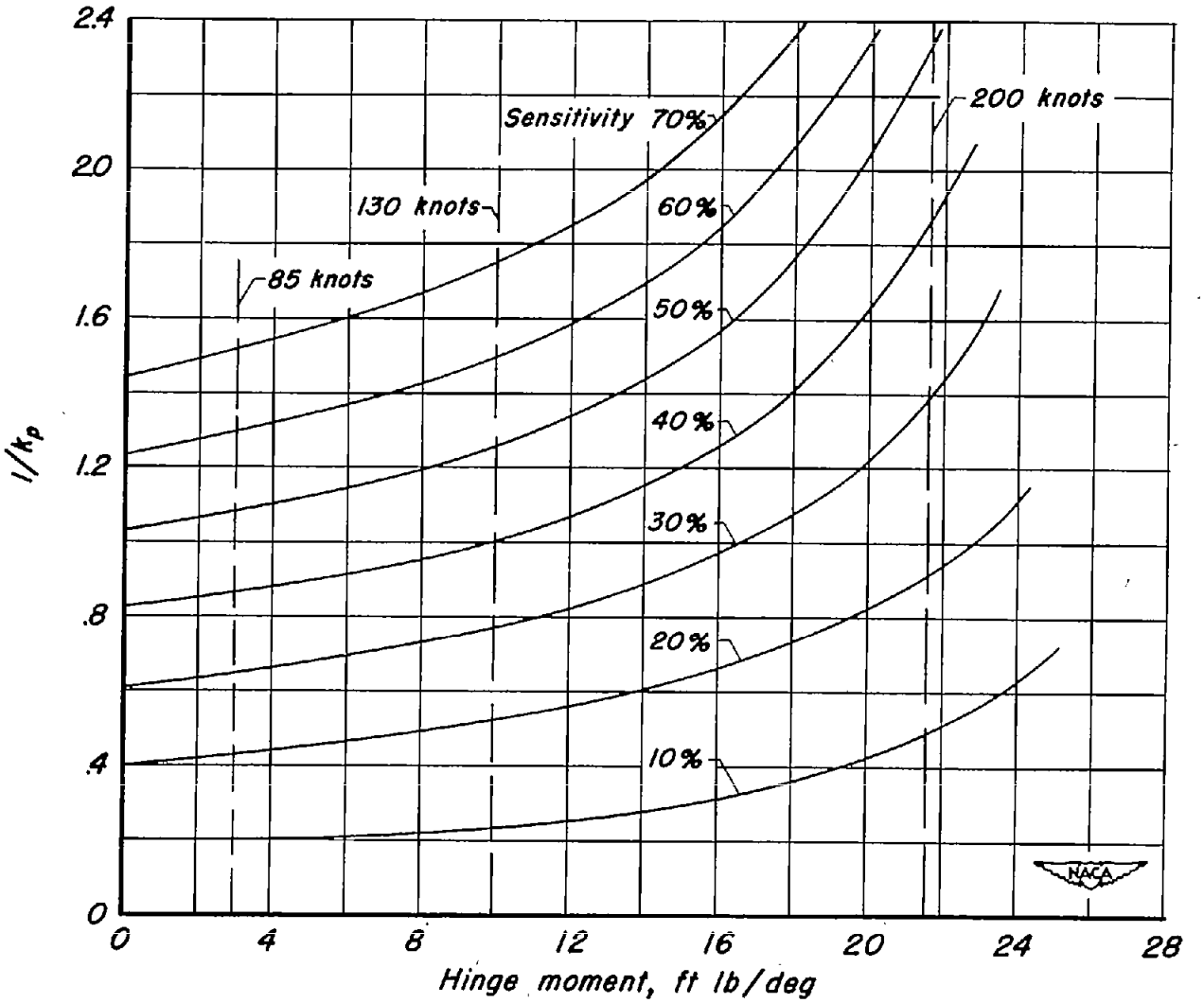

Figure 9.- Reciprocal gearing, $1/k_p$, versus hinge moment for various sensitivities.

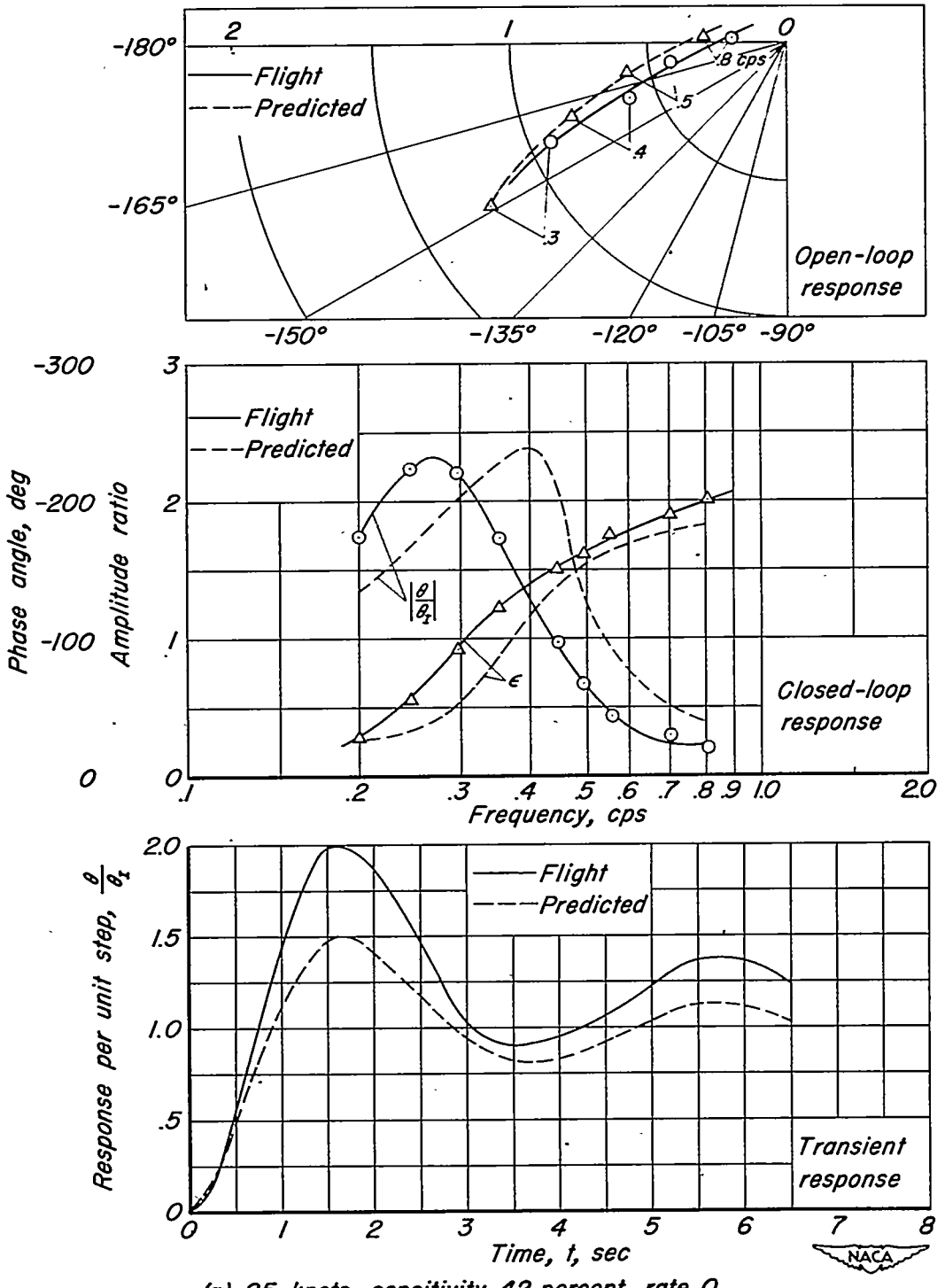

(a) 85 knots, sensitivity 42 percent, rate 0.

Figure 10.– Combined autopilot-airplane response.

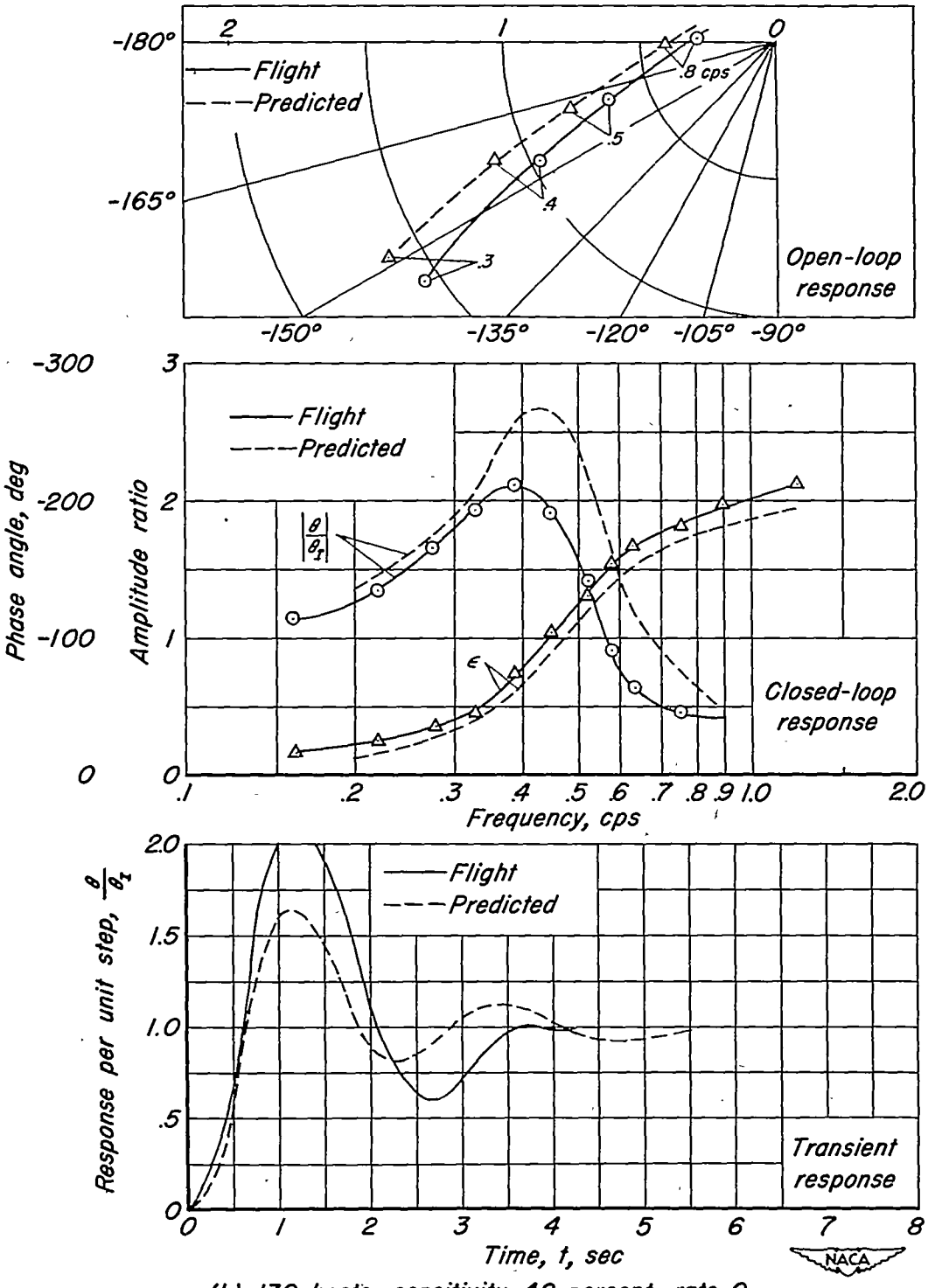

(b) 130 knots, sensitivity 42 percent, rate 0.

Figure 10.– Continued.

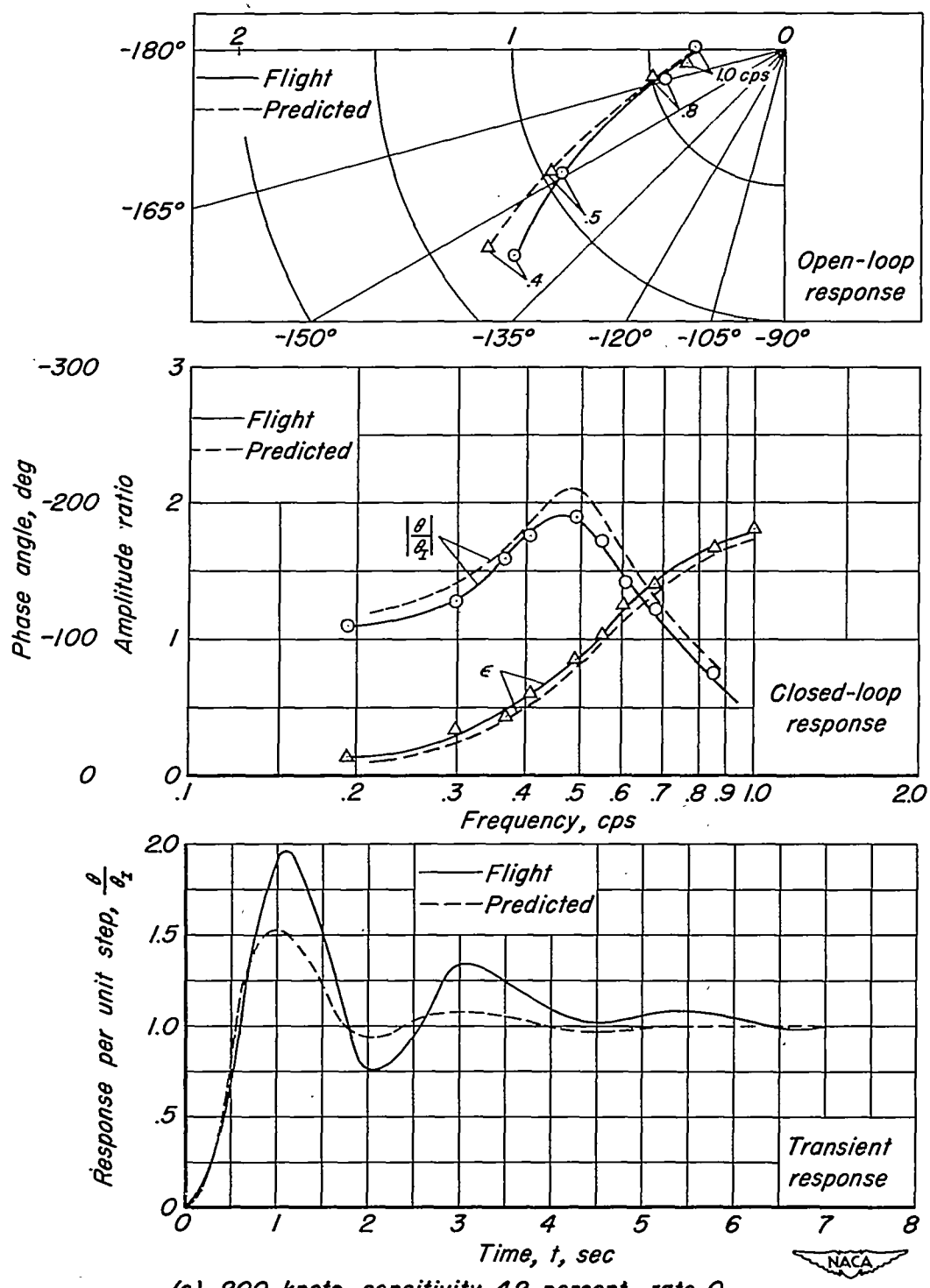

(c) 200 knots, sensitivity 42 percent, rate 0.

Figure 10.- Continued.

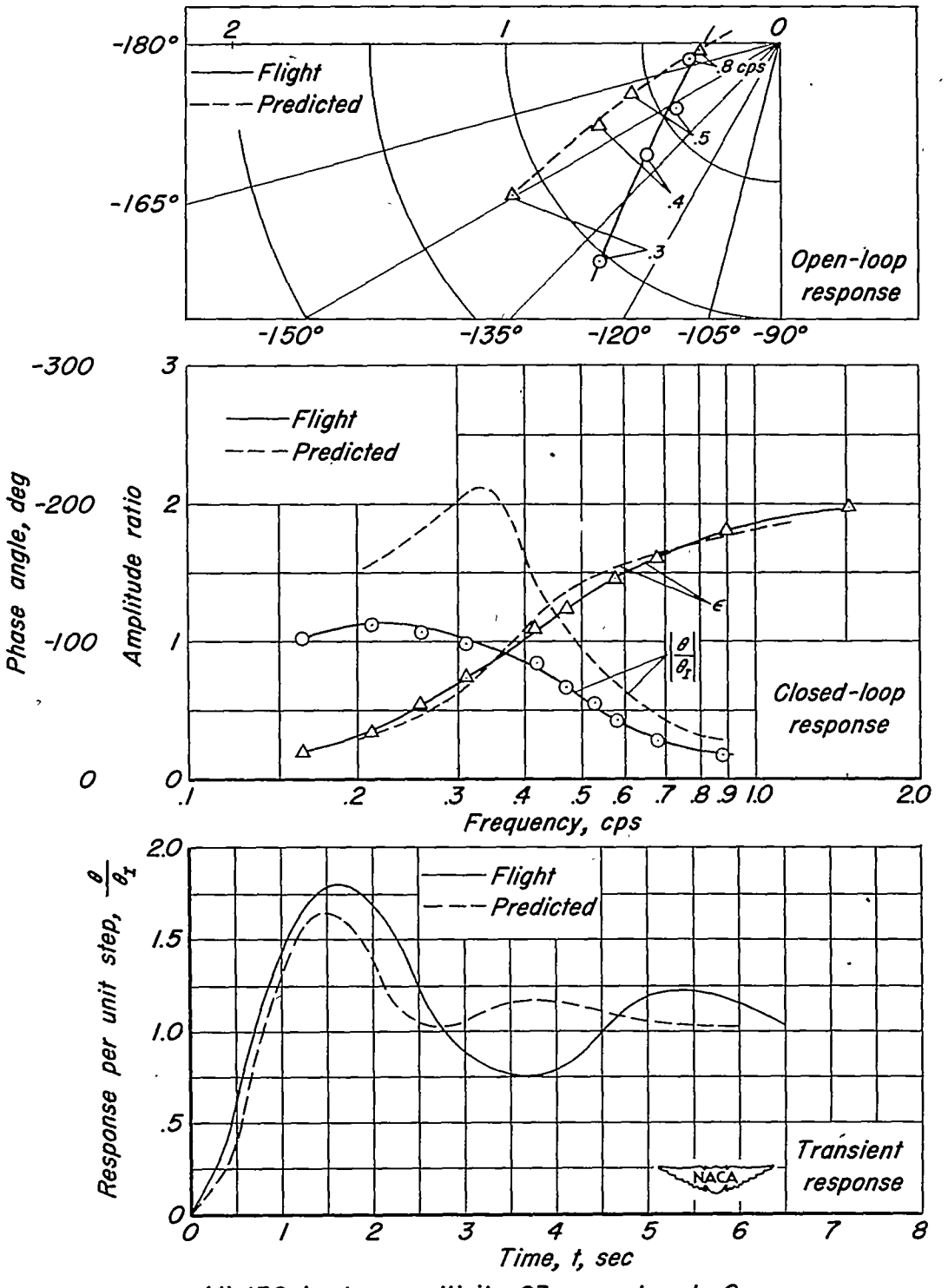

(d) 130 knots, sensitivity 63 percent, rate 0.

Figure 10.- Continued.

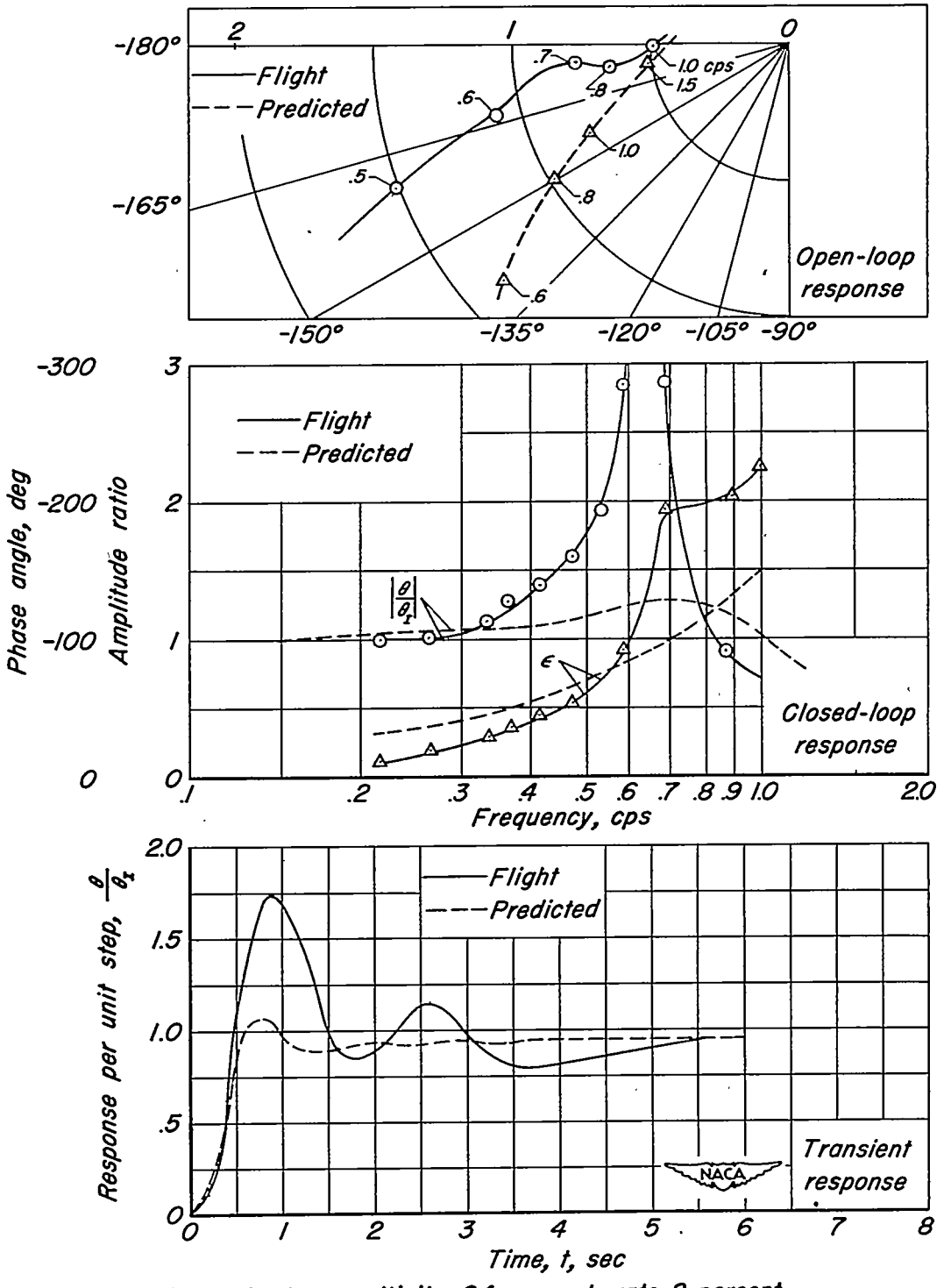

(e) 130 knots, sensitivity 24 percent, rate 8 percent.

Figure 10.– Continued.

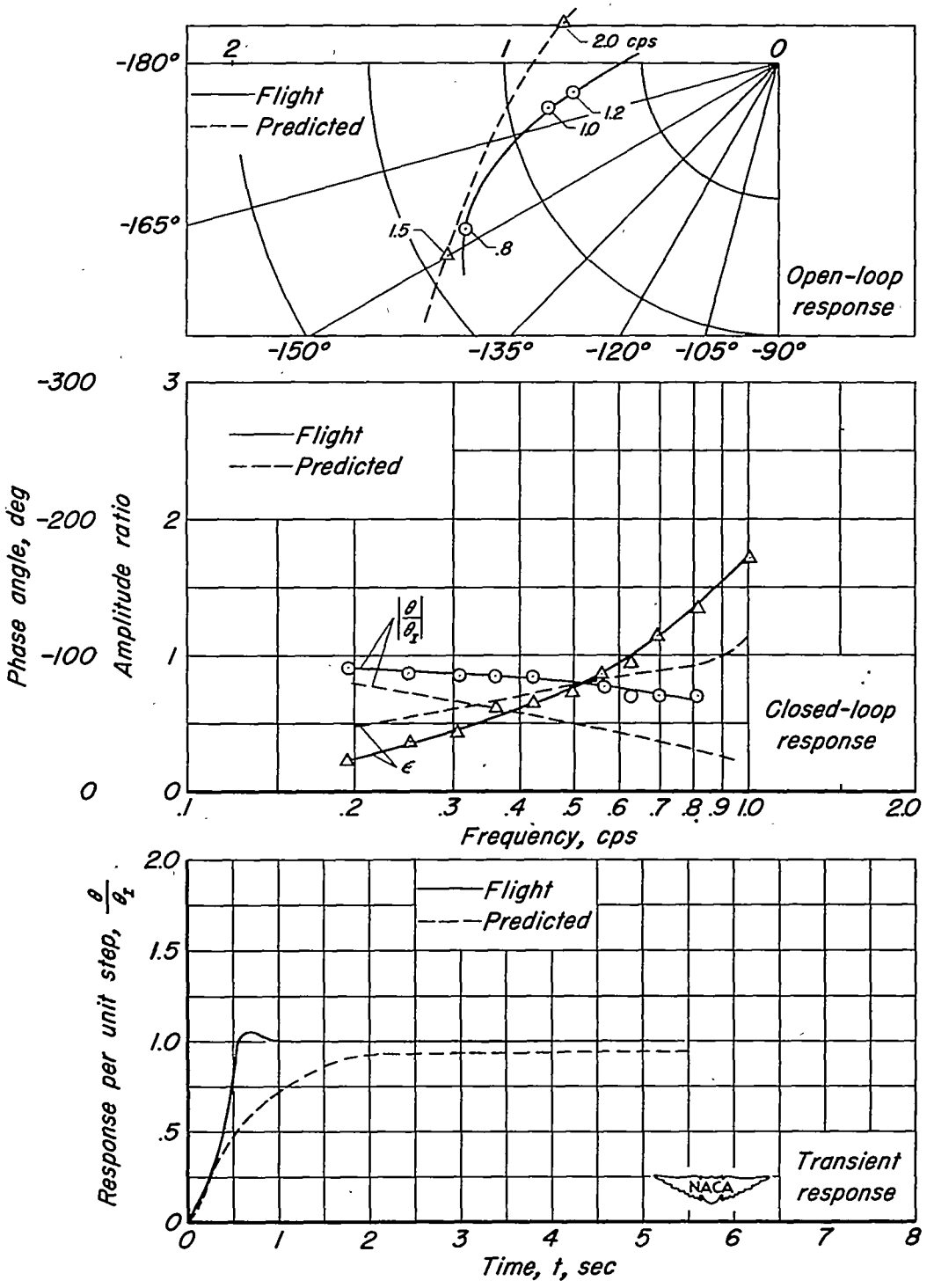

(f) 130 knots, sensitivity 24 percent, rate 31 percent.

Figure 10.- Continued.

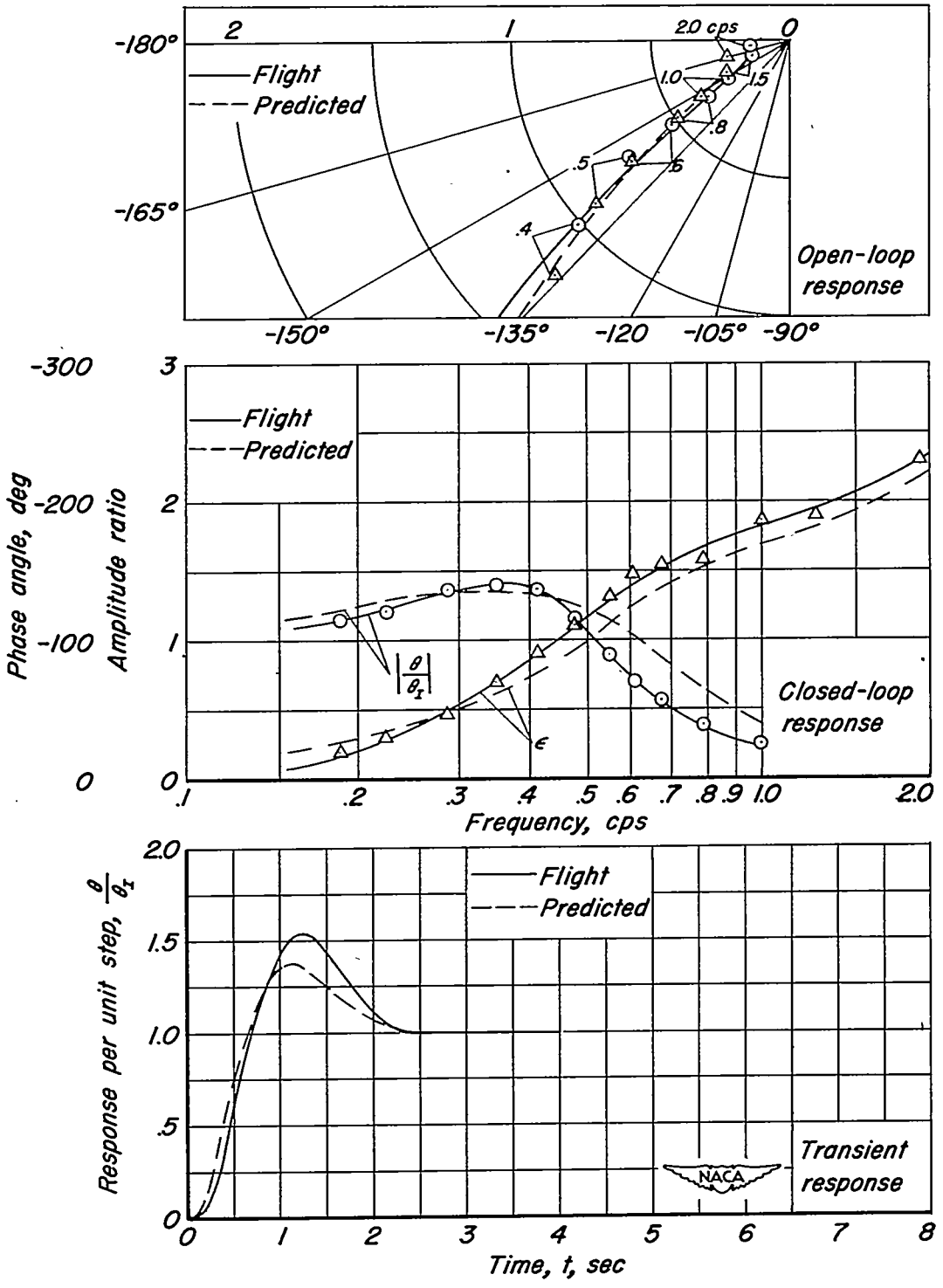

(g) 130 knots, sensitivity 42 percent, rate 8 percent.

Figure 10.- Continued.

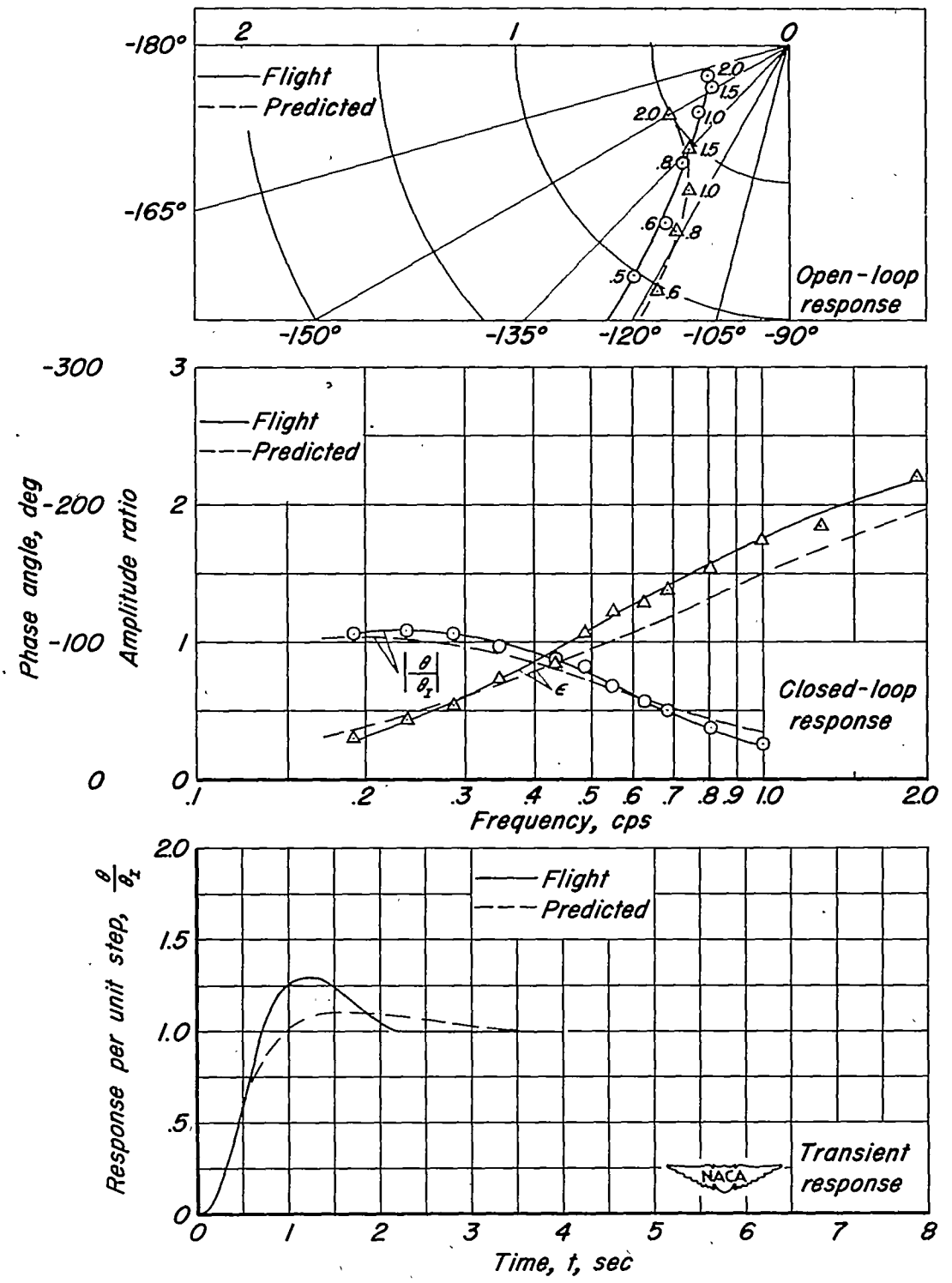

(h) 130 knots, sensitivity 42 percent, rate 20 percent.

Figure 10.- Continued.

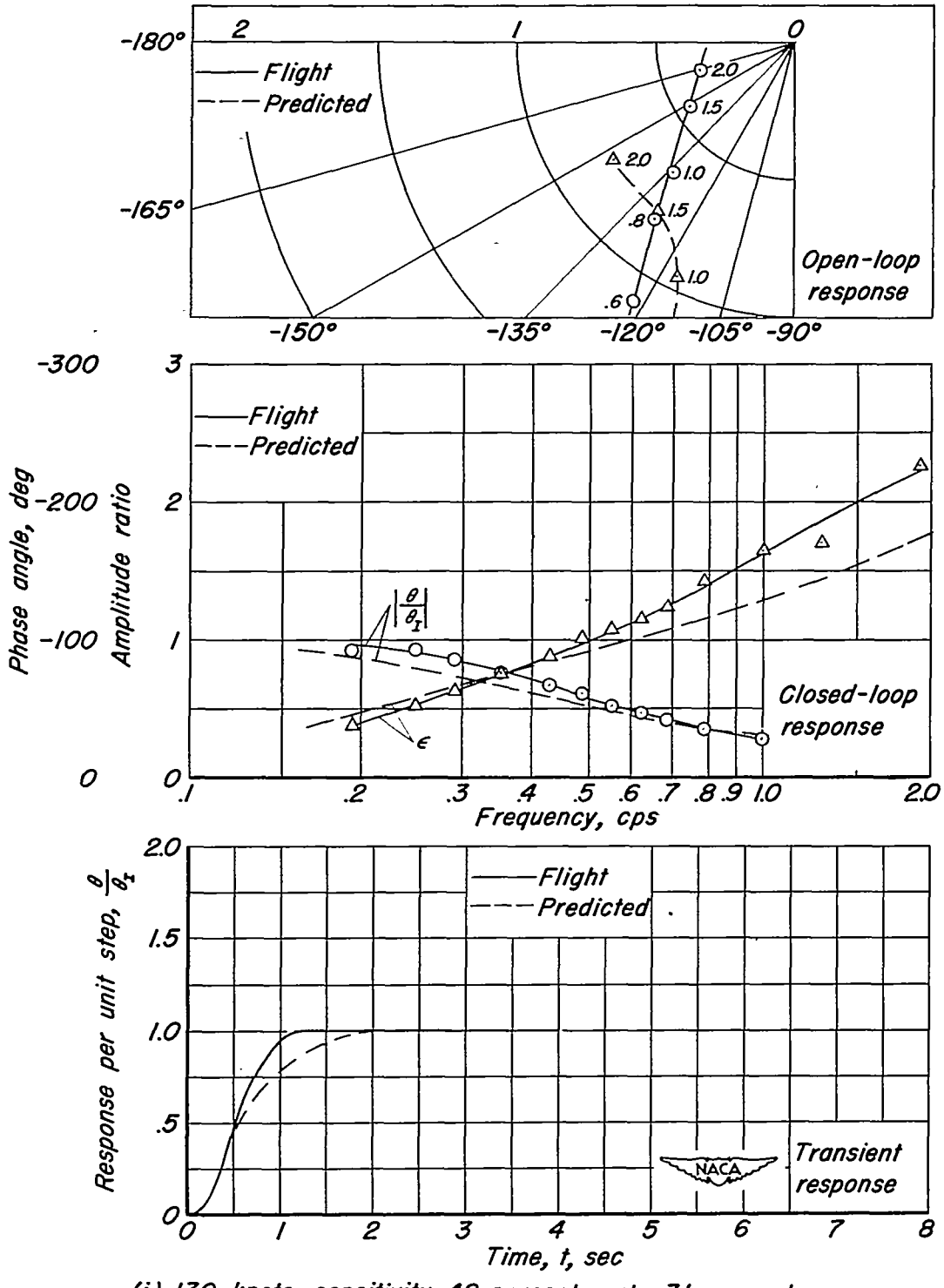

(i) 130 knots, sensitivity 42 percent, rate 31 percent.

Figure 10.- Concluded.

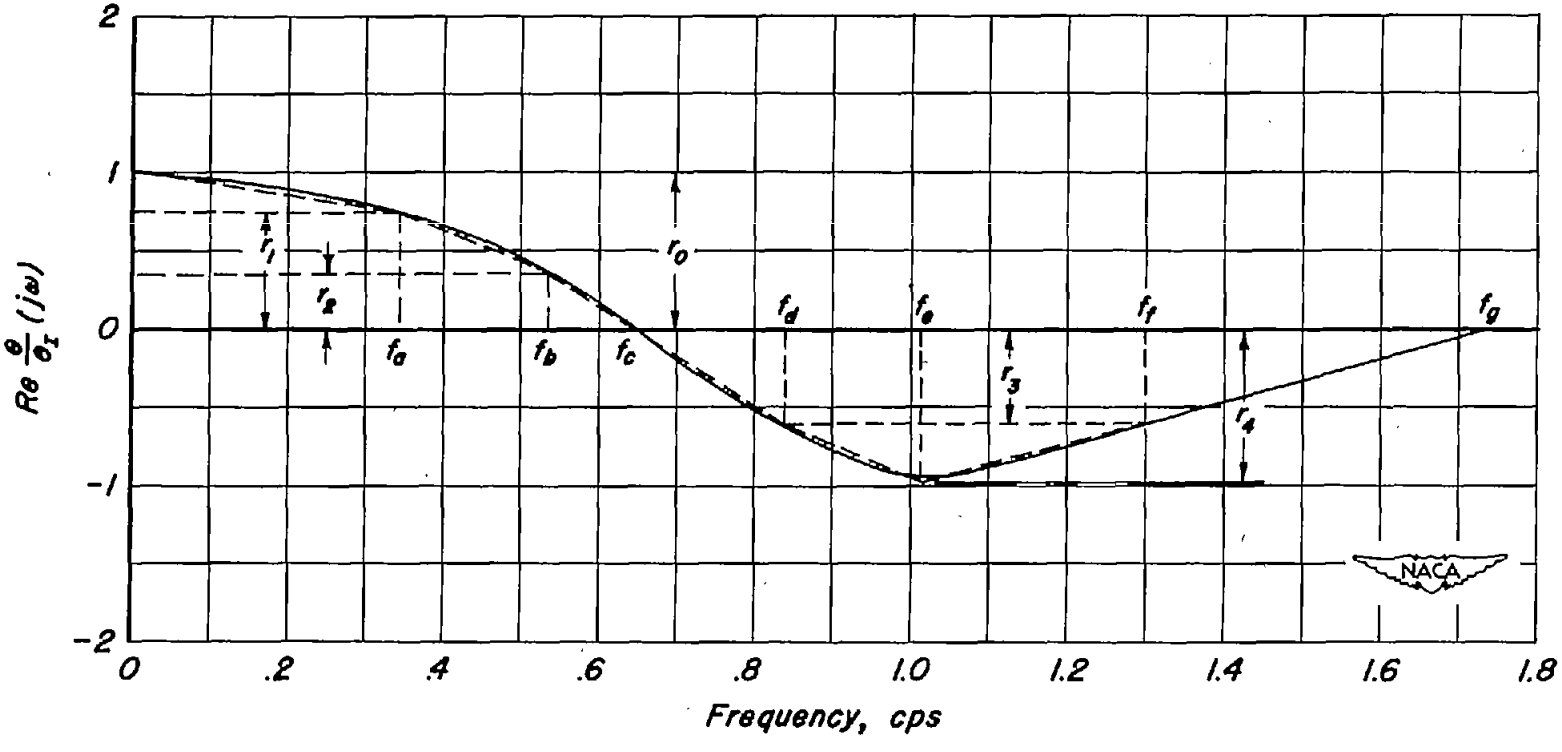

Figure 11.- Approximation of real part of closed-loop response, $Re\ \frac{\theta}{\theta_I}(j\omega)$, by several trapezoids for 130 knots, sensitivity 24 percent, and rate 8 percent.

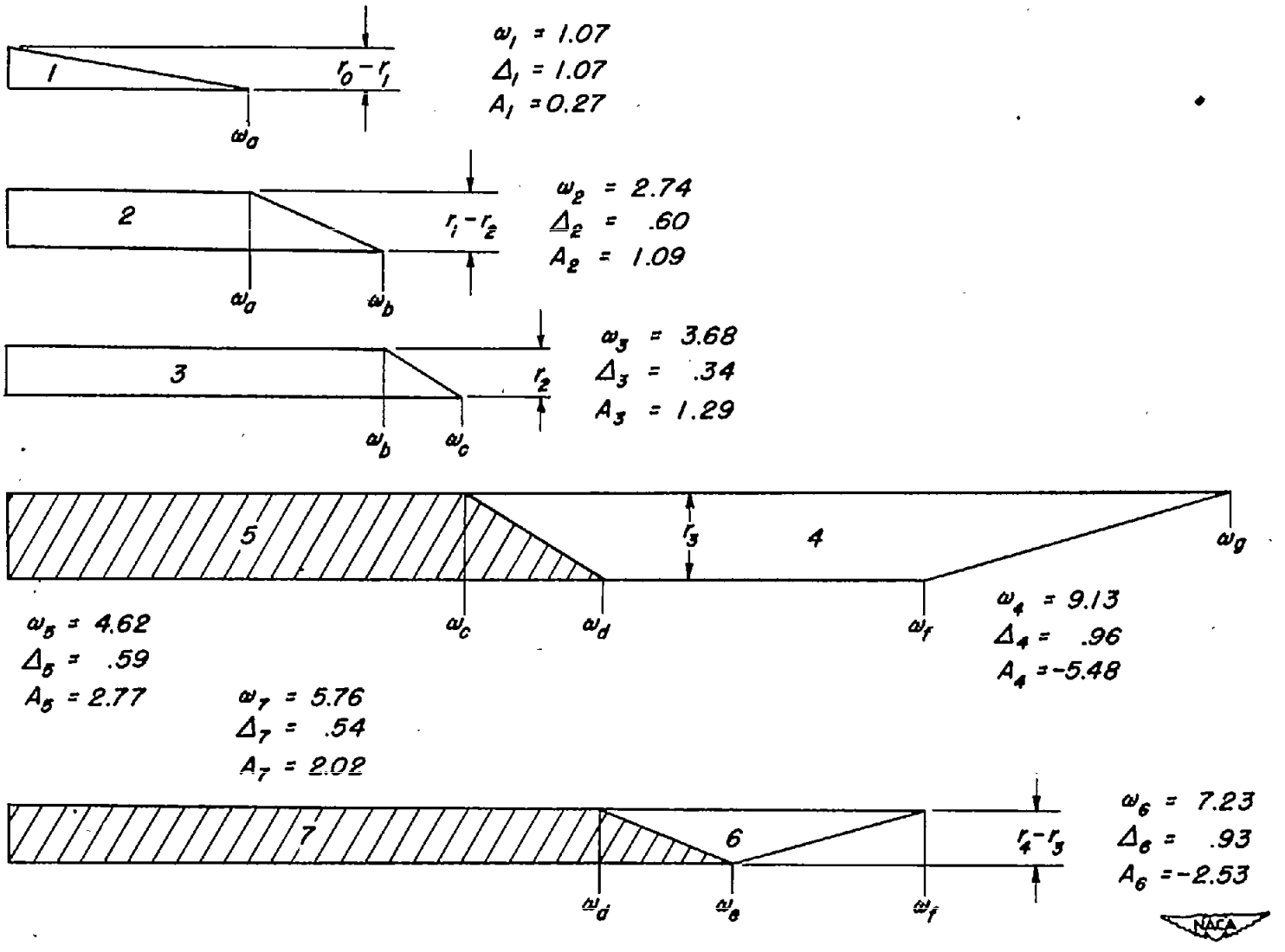

Figure 12.- Individual trapezoids required for approximation of real part of closed-loop response.

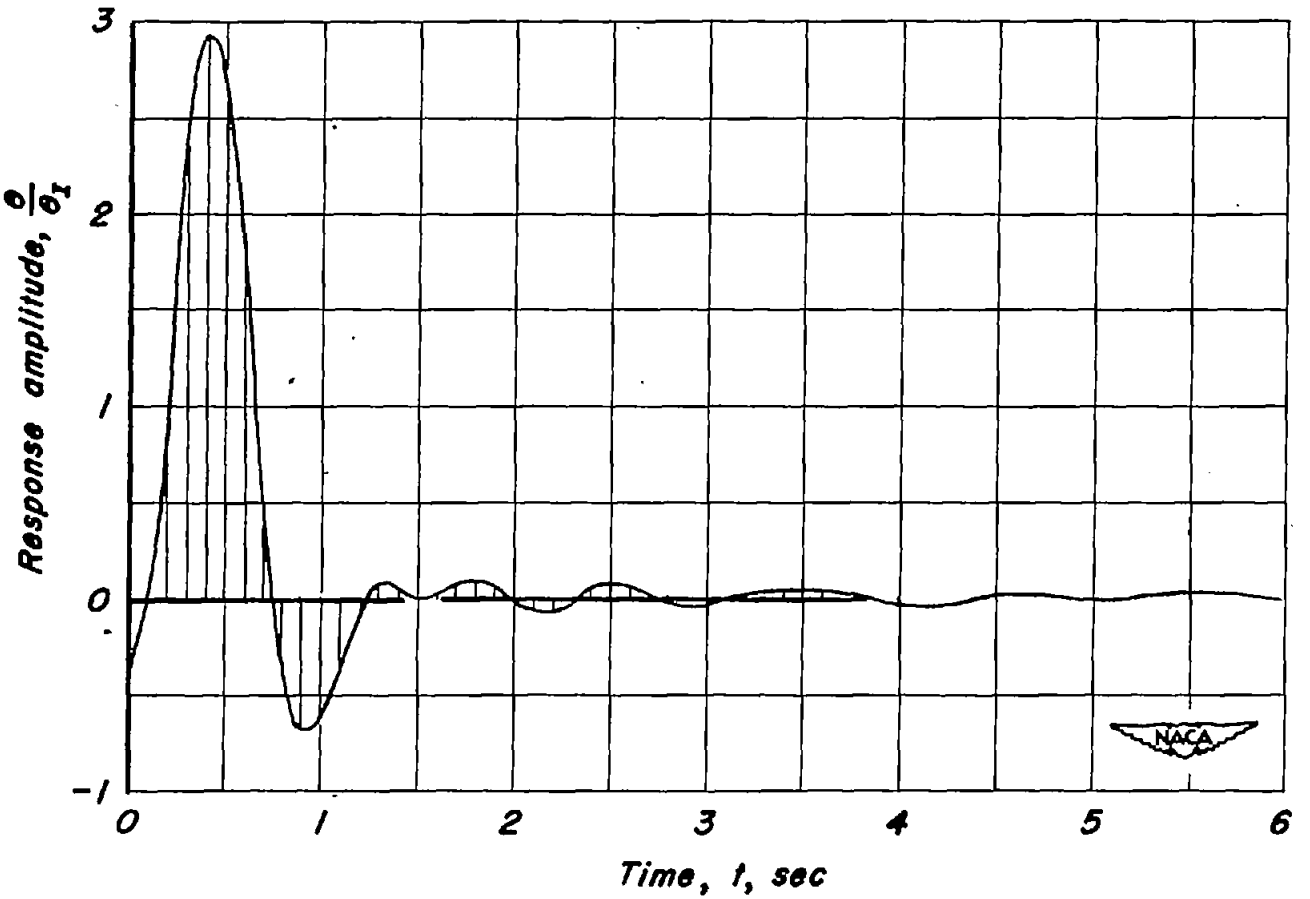

Figure 13.- Impulse response $\frac{\theta}{\theta_I}$ for 130 knots, sensitivity 24 percent, and rate 8 percent.